1968-03

A study to determine the effect of artificial tangential inertia on the dynamic response of elastic rings.

Hickman, Harold William

Monterey, California. Naval Postgraduate School

A STUDY TO DETERMINE THE EFFECT OF ARTIFICIAL TANGENTIAL INERTIA ON THE DYNAMIC RESPONSE OF ELASTIC RINGS

HAROLD WILLIAM HICKMAN

A STUDY TO DETERMINE THE EFFECT OF ARTIFICIAL TANGENTIAL INERTIA ON THE DYNAMIC RESPONSE OF ELASTIC RINGS

by

Harold William Hickman, Jr.
Ensign, United States Navy
B.S., United States Naval Academy, 1967

Submitted in partial fulfillment of the
requirements for the degree of

MASTER OF SCIENCE IN AERONAUTICAL ENGINEERING

from the

NAVAL POSTGRADUATE SCHOOL
March 1968

ABSTRACT

The elastic transient response of an impulsively loaded circular ring is examined. The numerical stability criterion associated with a finite difference formulation of the problem is briefly discussed, and a method to reduce the stability restriction is presented. This method assumes that the density of the ring is greater in the tangential direction than it is in the radial direction. The analytical solution to the ring equations with the artificial tangential inertia is determined for a specific impulsive load. This solution is compared with the solution to the ring equations with the correct tangential inertia. The comparison shows that on the basis of predicting peak values of stress, the results for the ring with the artificial tangential inertia are very close to those of the unmodified ring. Thus, the method reduces the numerical stability requirements and does not significantly affect the principal results.

TABLE OF CONTENTS

CHAPTER		PAGE
I.	INTRODUCTION	11
II.	A DISCUSSION OF THE RING EQUATIONS	15
III.	SOLUTION FOR THE IMPULSIVELY LOADED RING	20
IV.	SOLUTIONS FOR THE IMPULSIVELY LOADED MODIFIED RING	34
V.	CONCLUSIONS	49
REFERENCES		52
APPENDIX A	SOLUTION FOR THE SPECIFIC IMPULSE LOADING	53
APPENDIX B	CALCULATED FREQUENCY COEFFICIENTS	63

LIST OF TABLES

TABLE		PAGE
I.	Maximum Values for the Stress-Resultants	29
II.	Maximum Bending Moments	39
III.	Maximum Normal Force (Magnitudes)	39
IV.	Maximum Outer Edge Stress	39
V.	Frequency Coefficients ($\delta = 1$)	63
VI.	Frequency Coefficients ($\delta = 2$)	63
VII.	Frequency Coefficients ($\delta = 3$)	64
VIII.	Frequency Coefficients ($\delta = 4$)	64

LIST OF FIGURES

FIGURE		PAGE
1.	General Ring Geometry	16
2.	Ring Middle Surface	17
3.	Two-Dimensional Stress-Resultants	17
4.	Impulse Loading on the Ring	21
5.	Lower Mode Shapes	25
6.	Physical Ring Data	27
7.	Bending Moment Response at $\phi = 0$ ($\gamma = 1$)	30
8.	Normal Force and Edge Stress at $\phi = 0$ ($\gamma = 1$)	31
9.	Bending Moment Response at $\phi = \frac{\pi}{2}$ ($\gamma = 1$)	32
10.	Normal Force and Edge Stress at $\phi = \frac{\pi}{2}$ ($\gamma = 1$)	33
11.	Assumed Inertia Forces	35
12.	Change in $\bar{f}_n$ with γ	37
13.	Change in $\bar{g}_n$ with γ	37
14.	Bending Moment Response at $\phi = 0$ ($\gamma = 2$)	40
15.	Normal Force and Edge Stress at $\phi = 0$ ($\gamma = 2$)	41
16.	Bending Moment Response at $\phi = 0$ ($\gamma = 3$)	42
17.	Normal Force and Edge Stress at $\phi = 0$ ($\gamma = 3$)	43
18.	Bending Moment Response at $\phi = 0$ ($\gamma = 4$)	44
19.	Normal Force and Edge Stress at $\phi = 0$ ($\gamma = 4$)	45
20.	Bending Moment Response at $\phi = \frac{\pi}{2}$ ($\gamma = 2$)	46
21.	Bending Moment Response at $\phi = \frac{\pi}{2}$ ($\gamma = 3$)	47
22.	Bending Moment Response at $\phi = \frac{\pi}{2}$ ($\gamma = 4$)	48

TABLE OF SYMBOLS

A	Ring radius
A_n, B_n	Arbitrary functions of time
a_n, b_n	Arbitrary constants
D	Eh
E	Modulus of elasticity
f_n, g_n	Frequency coefficients for the original ring
$\bar{f}_n$, $\bar{g}_n$	Frequency coefficients for the modified ring
h	Ring thickness
I	Applied impulse
I_o	Maximum impulse
K	$\frac{Eh^3}{12}$
M	Circumferential bending moment
M_o	Non-dimensional bending moment for original ring
$\bar{M}_o$	Non-dimensional bending moment for modified ring
N	Circumferential normal force
N_o	Non-dimensional normal force for original ring
$\bar{N}_o$	Non-dimensional normal force for modified ring
n	Mode number
Q	Radial shear force
T	Time variable
V	Tangential displacement of the middle surface
W	Radial displacement of the middle surface
V_o	$\frac{I_o}{\rho h}$

Z	Radial coordinate
ρ	Ring density
γ	Artificial inertia factor
ϵ_ϕ	Circumferential strain at distance Z from middle
σ_o'	Non-dimensional stress (outer edge)
σ_i'	Non-dimensional stress (inner edge)
σ_ϕ	Circumferential stress at distance Z from middle
ϕ	Angular variable,
ω_n	Modal frequency

CHAPTER I

INTRODUCTION

The finite difference method of analysis has long been recognized as an effective and practical means for solving partial differential equations on a digital computer. The accuracy associated with this method can be adjusted by changing the incremental sizes of the independent variables involved. In the limit, when the sizes of the increments approach zero, the solution to the finite difference equations becomes identical to the solution to the corresponding differential equations. Consequently, the engineer may improve the accuracy of his finite difference solution by choosing sufficiently small values for the incremental sizes of the independent variables, with greater accuracy accompanied by increased execution time on the digital computer. However, there are many problems where the finite difference method imposes a restriction on the sizes of the increments. This restriction is known as the stability criterion and arises from a purely numerical phenomenon. The stability criterion defines a critical limit for the ratio of the increment sizes above which a numerically stable, valid solution will result. A value of the ratio below this limit will lead to a divergent, meaningless solution.

The stability criterion for the finite difference dynamic analysis of the thin, homogeneous, elastic, circular ring has been

defined by Ball.[1] It can be simplified to

$$\frac{A\Delta\phi}{\Delta T} \geq \sqrt{\frac{D}{\rho h}} \qquad (\Delta\phi)^2 << 1$$

where A is the radius of the ring; h is the thickness of the ring; D = Eh, the stretch rigidity; ρ is the ring density; and, $\Delta\phi$ and ΔT are the angular and time increments, respectively. A meaningful numerical solution for the transient response of the ring is possible only when the above restriction on $\Delta\phi$ and ΔT is observed. A physical interpretation of the stability criterion says that the finite difference solution must propagate around the ring at least as rapidly as a stress wave.

Once the size of $\Delta\phi$ is chosen, the maximum size for the time increment becomes

$$(\Delta T)_{MAX} = (\Delta\phi)\, A \sqrt{\frac{\rho h}{D}} \qquad (1)$$

An accurate solution for the ring response requires a small value for the angular increment, $\Delta\phi$. Therefore, according to Equation (1), $(\Delta T)_{MAX}$ is automatically restricted to a small value; and hence, large computation times will be required on the computer.

To reduce the restrictions on the numerical stability of the ring response a method is proposed whereby the maximum time increment may be increased without producing an unstable solution. According

to Equation (1), $(\Delta T)_{MAX}$ is determined once $\Delta\phi$ is chosen. However, if the density ρ is considered to be a variable in the stability criterion then $(\Delta T)_{MAX}$ will be proportional to the square root of the density at a particular value for $\Delta\phi$. The density in Equation (1) is a measure of the ring's inertia in the direction of the propagation of stress disturbances around the ring, that is, the tangential direction. The method proposed here modifies the ring by introducing an artificial tangential density that is larger than the actual ring density. Thus, the ring inertia will be characterized by the density ρ in the radial direction and by a different density, $\gamma\rho$, in the tangential direction. At a given value of $\Delta\phi$, the maximum time increment for a stable response of the modified ring will be proportional to the square root of $\gamma\rho$ and, hence, will be larger than the critical time increment for the original ring by the factor $\sqrt{\gamma}$.

For example, for $\gamma = 4$ the time increment for stable response of the modified ring is twice as large as the time increment for the original ring for the same $\Delta\phi$. Thus, the computation time can be cut in half. The decreased computational time afforded by the proposed method is a significant improvement on the conventional finite difference method of analysis. However, the introduction of the artificial tangential inertia will also lead to an incorrect solution for the ring response. Thus, the value of the method will depend upon the accuracy of the solution of the modified ring.

This paper investigates the effect of an artificial tangential inertia on the analytical solution for a particular ring problem. Solutions are obtained for the elastic response of an impulsively loaded circular ring with and without artificial tangential inertia. The maximum stress in the ring is computed for the original ring ($\gamma = 1$) and for rings with $\gamma = 2$, 3, and 4. A comparison of the maximum stress for each ring demonstrates the value of the method.

This study was completed during the 1967-1968 academic year at the Naval Postgraduate School, Monterey, California. Acknowledgement is gratefully made to Professor Robert E. Ball of the Aeronautics Department for his guidance and consultation.

CHAPTER II

A DISCUSSION OF THE RING EQUATIONS

This thesis considers a thin, circular ring composed of a homogeneous material. The governing equations are derived in Reference 4 and are repeated here for completeness. Figures 1 and 2 illustrate the general geometrical characteristics. The radius A is measured to the middle surface of the ring, which lies at a distance $\frac{h}{2}$ from both edges. A differential element on the ring, $d\phi$, is located at an angle ϕ from the bottom of the ring, where ϕ is measured positive counter-clockwise. The displacement of a point on the middle surface is described by a radial and a tangential component, W and V, respectively. The radial distance from the middle surface to some arbitrary point on the ring is given by Z in Figure 2.

A two-dimensional problem will be assumed with regard to the internal stresses of the ring. Figure 3 illustrates the forces acting on the element $d\phi$ due to the normal and shear stress distributions on the cross-sections. The forces N, M, and Q are, respectively, the normal force, the bending moment, and the radial shear force. These forces are stress-resultants referred to the middle surface of the element. The definitions of N and M are given by the following expressions

$$N = \int_{-\frac{h}{2}}^{\frac{h}{2}} \sigma_\phi \, dZ = \int_{-\frac{h}{2}}^{\frac{h}{2}} E \epsilon_\phi \, dZ \qquad (2a)$$

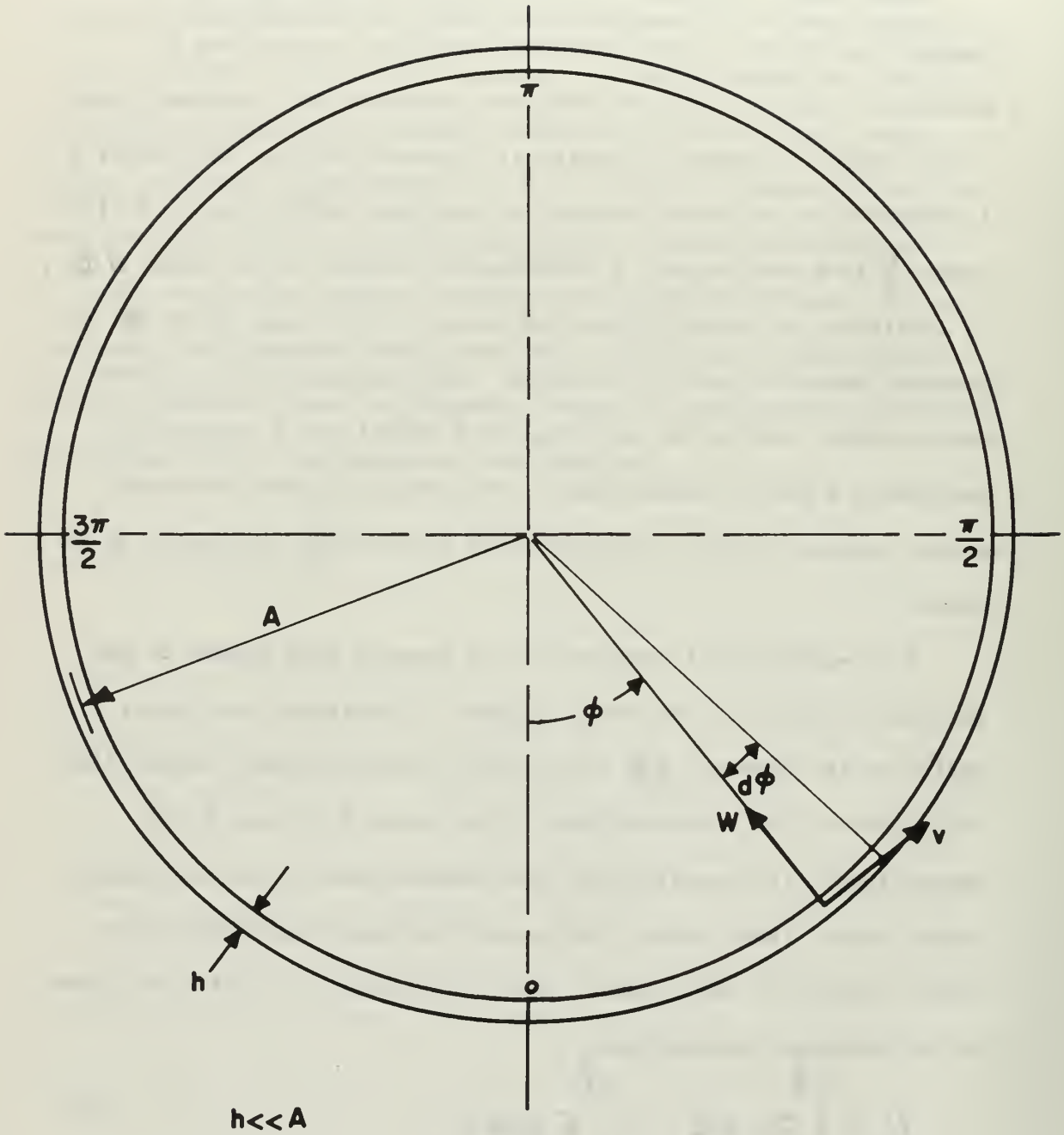

FIG. 1

GENERAL RING GEOMETRY

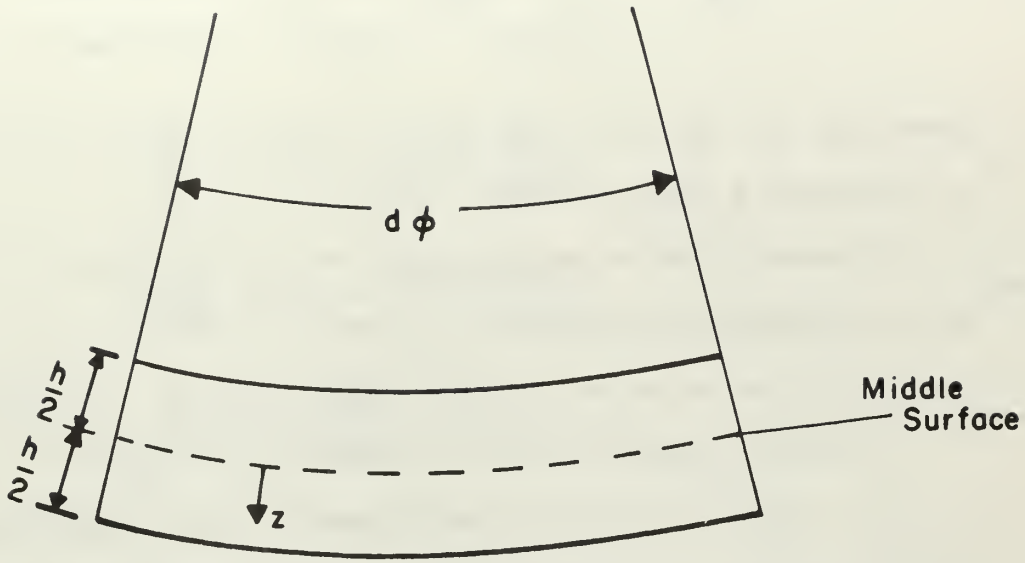

FIG. 2

RING MIDDLE SURFACE

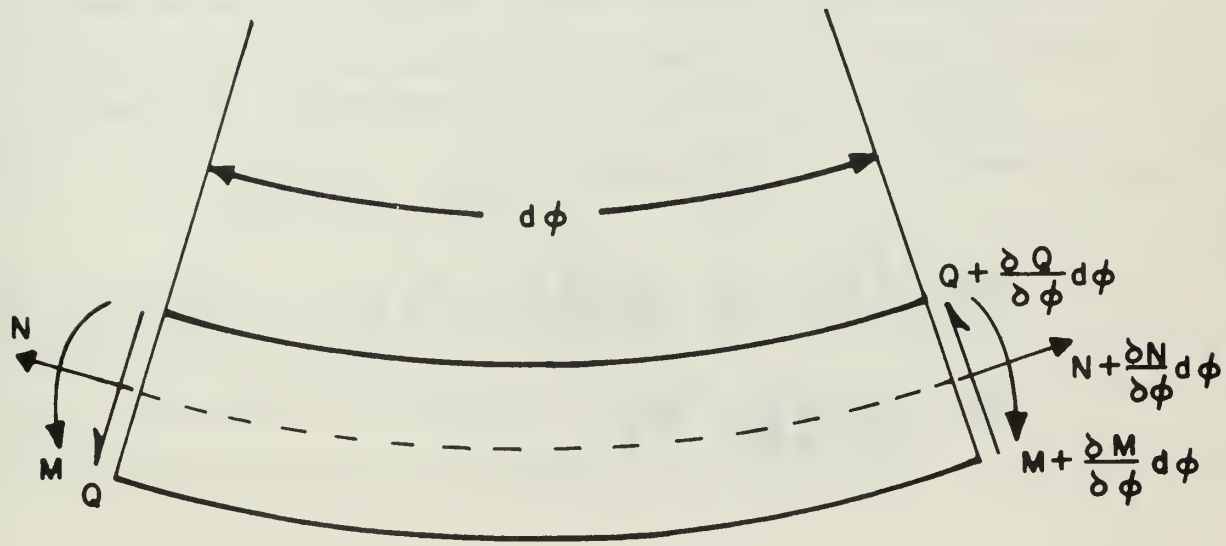

FIG. 3

TWO-DIMENSIONAL STRESS-RESULTANTS

$$M = \int_{-\frac{h}{2}}^{\frac{h}{2}} \sigma_\phi \, Z \, dz = \int_{-\frac{h}{2}}^{\frac{h}{2}} E \epsilon_\phi \, Z \, dz \tag{2b}$$

where σ_ϕ and ϵ_ϕ are the stress and strain on the cross section at a distance Z from the middle surface.

In order to obtain an expression for the strain ϵ_ϕ in terms of Z, two additional assumptions are made:

1. A line normal to the middle surface before deformation will be normal to this surface after deformation.
2. A point on the normal to the middle surface will have a constant distance Z from this surface, both before and after deformation.

Accordingly,

$$\epsilon_\phi = \frac{1}{A} \frac{\partial V}{\partial \phi} + \frac{Z}{A(A+Z)} \frac{\partial^2 W}{\partial \phi^2} - \frac{W}{A+Z} \tag{3}$$

Substituting Equation (3) into the definitions for N and M, Equations (2a) and (2b), leads to

$$N = \frac{D}{A}\left(\frac{\partial V}{\partial \phi} - W\right) - \frac{K}{A^3}\left(\frac{\partial^2 W}{\partial \phi^2} + W\right) \tag{4}$$

$$M = -\frac{K}{A^2}\left(\frac{\partial^2 W}{\partial \phi^2} + W\right) \tag{5}$$

where $D = Eh$ $\qquad K = \frac{Eh^3}{12}$

The linear equilibrium equations for the element follow directly from an examination of Figure 3. They are

$$\frac{\partial N}{\partial \phi} - Q = \rho A h \frac{\partial^2 V}{\partial T^2} \tag{6a}$$

$$\frac{\partial Q}{\partial \phi} + N = \rho A h \frac{\partial^2 W}{\partial T^2} \tag{6b}$$

$$Q - \frac{1}{A}\frac{\partial M}{\partial \phi} = 0 \tag{6c}$$

where rotary inertia is neglected.

Eliminating the radial shear Q from these equations leads to

$$\frac{\partial N}{\partial \phi} - \frac{1}{A}\frac{\partial M}{\partial \phi} = \rho A h \frac{\partial^2 V}{\partial T^2} \tag{7a}$$

$$\frac{1}{A}\frac{\partial^2 M}{\partial \phi^2} + N = \rho A h \frac{\partial^2 W}{\partial T^2} \tag{7b}$$

Substituting Equations (4) and (5), relating the stress-resultants to the displacements W and V, into Equations (7a) and (7b), gives

$$\frac{D}{A}\left(\frac{\partial^2 V}{\partial \phi^2} - \frac{\partial W}{\partial \phi}\right) = \rho A h \frac{\partial^2 V}{\partial T^2} \tag{8a}$$

$$\frac{K}{A^3}\left(\frac{\partial^4 W}{\partial \phi^4} + 2\frac{\partial^2 W}{\partial \phi^2} + W\right) - \frac{D}{A}\left(\frac{\partial V}{\partial \phi} - W\right) = -\rho A h \frac{\partial^2 W}{\partial T^2} \tag{8b}$$

These are the differential equations that describe the free vibrations of the thin, two-dimensional, elastic ring.

CHAPTER III

SOLUTION FOR THE IMPULSIVELY LOADED RING

In order to adequately test the proposed method for increasing the critical time step, an impulsive load that causes both large bending and membrane stresses should be employed. Consequently, the impulsive load illustrated in Figure 4 is taken as the loading on the ring at time t = 0. The impulse is applied to the top half of the ring and is characterized by a cosine distribution directed radially inward.

The initial conditions for the radial cosine impulse are given by

$$W(\phi, 0) = 0 \qquad V(\phi, 0) = 0$$

$$\frac{\partial V}{\partial T}(\phi, 0) = 0$$

$$\frac{\partial W}{\partial T}(\phi, 0) = -V_0 \cos\phi \qquad \frac{\pi}{2} \leq \phi \leq \frac{3\pi}{2}$$

$$= 0 \qquad -\frac{\pi}{2} \leq \phi \leq \frac{\pi}{2} \qquad (9)$$

where $$V_0 = \frac{I_0}{\rho h}$$

Since the ring is unrestrained, a net momentum will be imparted by the radial velocity acting on the upper half of the ring. This will cause a rigid body translation of the ring, and hence, unbounded

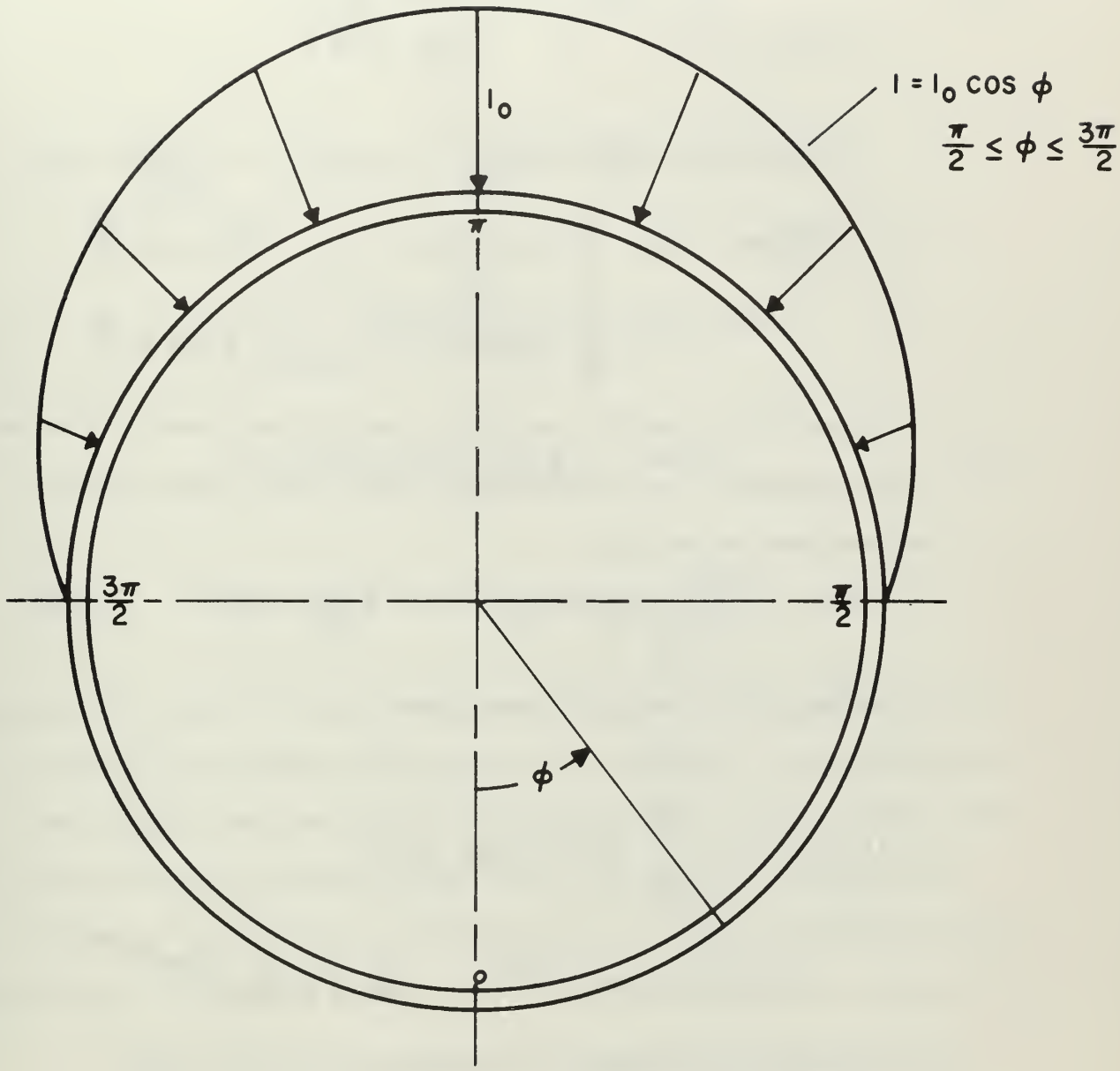

FIG. 4

IMPULSE LOADING ON THE RING

values for the displacements V and W. To avoid this situation, the initial conditions must be modified in such a way that the rigid body motion is eliminated, while preserving the internal effect of the impulse. Reference 2 defines the following modified set of initial conditions for this loading

$$W(\phi, 0) = 0 \qquad V(\phi, 0) = 0$$

$$\frac{\partial V}{\partial T}(\phi, 0) = \frac{V_0}{4} \sin \phi$$

$$\frac{\partial W}{\partial T}(\phi, 0) = -\frac{3}{4} V_0 \cos \phi \qquad \frac{\pi}{2} \leq \phi \leq \frac{3\pi}{2}$$

$$= \frac{V_0}{4} \cos \phi \qquad -\frac{\pi}{2} \leq \phi \leq \frac{\pi}{2} \tag{10}$$

With this set of initial conditions, the ring will remain fixed in space; and hence, the displacements V and W will measure actual deformations of the ring.

The following solutions for W and V are assumed

$$W(\phi, T) = \sum_{n=0}^{\infty} A_n(T) \cos n\phi \tag{11a}$$

$$V(\phi, T) = \sum_{n=1}^{\infty} B_n(T) \sin n\phi \tag{11b}$$

$$A_n(T) = a_n e^{i\omega_n T} \qquad B_n(T) = b_n e^{i\omega_n T} \; * \tag{12}$$

*a_n and b_n are arbitrary constants.

Based upon these solutions and the given initial conditions the expressions for the bending moment and normal force are*

$$M_o = -M\frac{A^2\omega_o\pi}{KV_o} = SIN\,\omega_o T + \sum_{n=2,4,\ldots}^{\infty} \frac{-2(-1)^{\frac{n}{2}+1}}{(f_n^2 - g_n^2)}\left[\frac{f_n^2 - n^2}{f_n} SIN\, f_n\omega_o T + \frac{n^2 - g_n^2}{g_n} SIN\, g_n\omega_o T\right] COS\, n\phi \qquad (13a)$$

$$N_o = N\frac{A\omega_o\pi}{DV_o} = -SIN\,\omega_o T + \frac{\pi}{2\sqrt{2}} SIN\sqrt{2}\,\omega_o T\, COS\,\phi + \sum_{n=2,4,\ldots}^{\infty} \frac{2(-1)^{\frac{n}{2}+1}}{(n^2-1)(f_n^2 - g_n^2)}\left[-f_n SIN\, f_n\omega_o T + g_n SIN\, g_n\omega_o T\right] COS\, n\phi - \alpha M_o \qquad (13b)$$

where $\alpha = \frac{K}{DA}$ $\qquad$ $\omega_o = \frac{1}{A}\sqrt{\frac{D}{\rho h}}$

M_o and N_o are non-dimensional representations of the bending moment and the normal force, both of which may be solved without specifying the impulse magnitude, I_o. The other terms will be described later. Equations (13a) and(13b) characterize the dynamic response of the elastic ring due to the specified impulse. Before proceeding further, however, a physical interpretation will be given to these expressions.

*These expressions are derived in Appendix A. Since this is the original ring, $\gamma = 1$.

Consider, first, the various mode shapes excited by the impulsive loading. Figure 5 illustrates the lower modes of vibration for the ring. The lowest mode, $n = 0$, is characterized by a radial displacement only, where W is the same for all points. A small change in curvature in addition to the middle surface straining will result; and hence, $N_\circ$ and $M_\circ$ will both have contributions from this mode as can be seen from Equations (4) and (5). The next mode, $n = 1$, involves middle surface straining only. The shape of the ring remains the same, with no change in the effective curvature of the ring. Hence, this mode will contribute only to the normal force, $N_\circ$. For $n > 1$, only the even mode shapes appear in the expressions for the stress-resultants. This situation arises from the modified initial conditions imposed on the ring. At time $t = 0$, positive radial velocities are required at the top and bottom of the ring, $\phi = \pi$ and 0, while zero radial velocities are prescribed at the sides, $\phi = \pm \frac{\pi}{2}$. Referring to Figure 5, it can be seen that only the even modes can account for these velocities and hence, are the only ones excited by the impulse.

Finally, examination of Equations (13a) and (13b) reveals that two frequencies, $f_n \omega_\circ$ and $g_n \omega_\circ$, are associated with each mode of vibration of the ring. These frequencies arise from the fact that the ring element, $d\phi$, may displace independently in two separate directions. From Appendix A, the frequency coefficients, f_n and g_n, are approximately given by

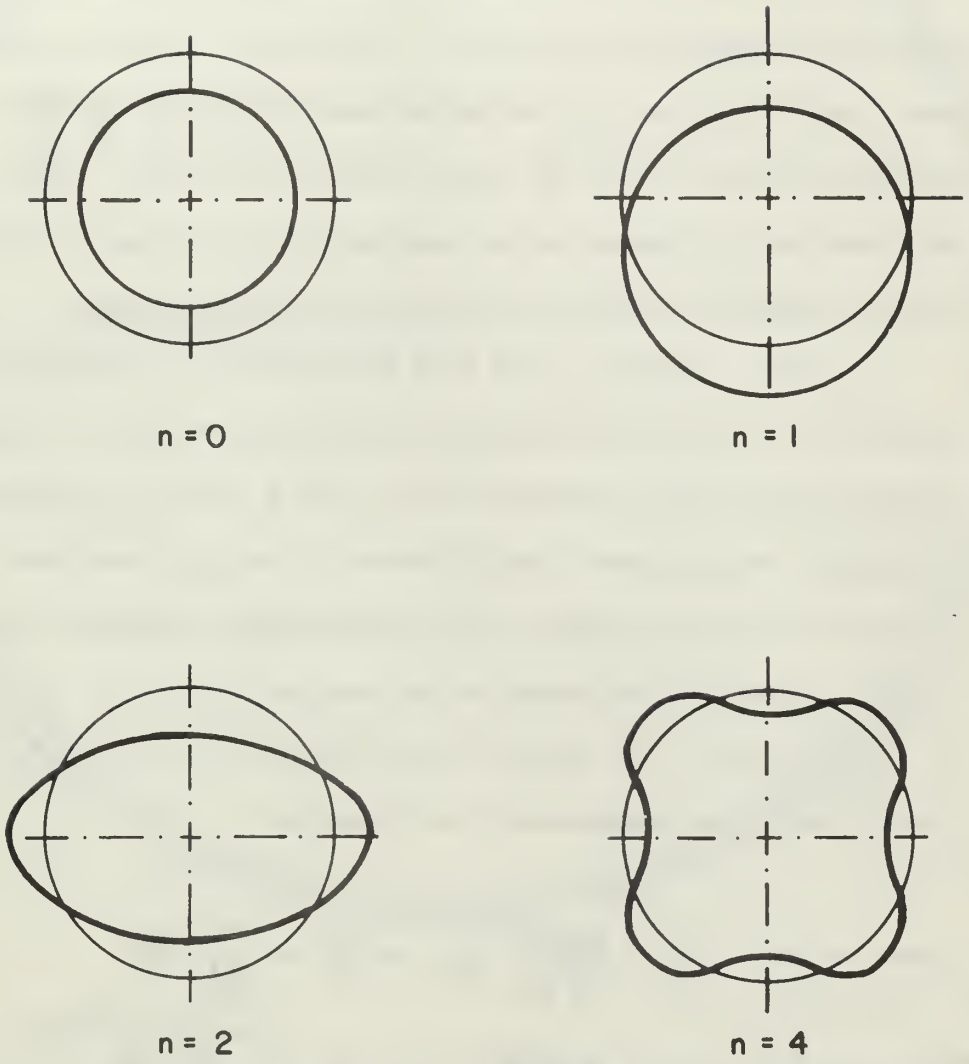

FIG. 5

LOWER MODE SHAPES

$$f_n \doteq n(n^2-1)\sqrt{\frac{\alpha}{n^2+1}}$$

$$g_n \doteq \sqrt{n^2+1} \qquad (14)$$

Since a thin ring is assumed, α is very small, and $f_n << g_n$. The frequency coefficients, f_n and g_n, characterize, respectively, the radial and tangential vibrations of the ring. Due to the relative magnitudes of f_n and g_n, the expressions for M_o and N_o will each be dominated by one of the two sine terms of the series. Hence, M_o will vary at a frequency given approximately by $f_n\omega_o$, while N_o will be characterized by a much larger frequency $g_n\omega_o$.

To obtain numerical data from Equations (13a) and (13b), it is necessary to select physical data describing the ring. Figure 6 outlines the physical characteristics for a thin ring composed of aluminum. The frequency coefficients, f_n and g_n, have been calculated on a digital computer at 20 micro-second intervals over a period of time corresponding to one complete cycle for M_o. Stresses on the inner and outer edges of the ring were also calculated from the following non-dimensional relationships

(outer edge) $$\sigma_o' = \frac{A\omega_o\pi}{EV_o}\sigma_o = N_o + \frac{h}{2A}M_o \qquad (15a)$$

(inner edge) $$\sigma_i' = \frac{A\omega_o\pi}{EV_o}\sigma_i = N_o - \frac{h}{2A}M_o \qquad (15b)$$

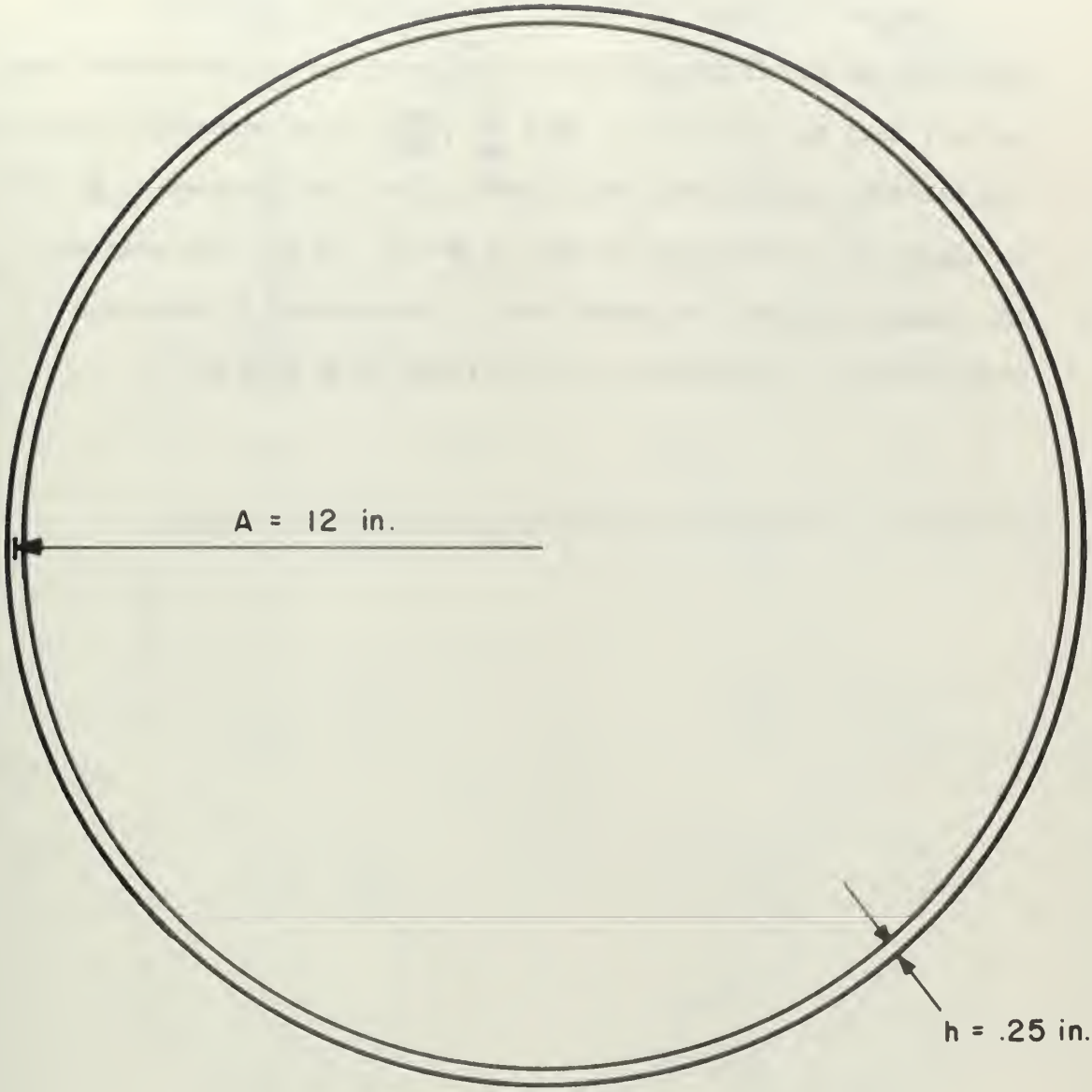

ω_o = 16980 rad./sec.

D = 2.74×10^6 lbf./in.

E = 10.9×10^6 lbf./in.^{2}

K = 1.43×10^4 lbf.-in.

ρ = 3.14×10^{-4} $\frac{\text{slugs}}{\text{in.}^3}$

α = 3.54×10^{-5}

FIG. 6

PHYSICAL RING DATA

The maximum values for M_o , N_o , and σ_o' found over the time sampled have been listed in Table I.*

Figures 7 through 10 illustrate the dynamic response of the ring through the first half cycle of M_o .** It should be noted from Table I that the response at $\phi = \frac{\pi}{4}, \frac{3\pi}{4}$ is of secondary importance and has been omitted from the curves. Also, the response at $\phi = \pi$ is identical in character to that at $\phi = 0$ and has been omitted. The symmetry of the even modes make it unnecessary to determine solutions for ring locations in the range $\pi \leq \phi \leq 2\pi$.

*The maximum σ_i' was observed to be within a few per cent of the maximum σ_o' found.

**A positive M_o indicates a negative bending moment.

TABLE I

MAXIMUM VALUES FOR THE STRESS-RESULTANTS

Φ	$\lvert N_{o_{MAX}} \rvert$	$M_{o_{MAX}}$	$\sigma'_{o_{MAX}}$
0	2.22	-129.6	-3.45
$\frac{\pi}{4}$	1.80	26.5	1.99
$\frac{\pi}{2}$	1.31	125.8	2.57
$\frac{3\pi}{4}$	1.77	26.5	1.80
π	2.39	-129.6	-3.27

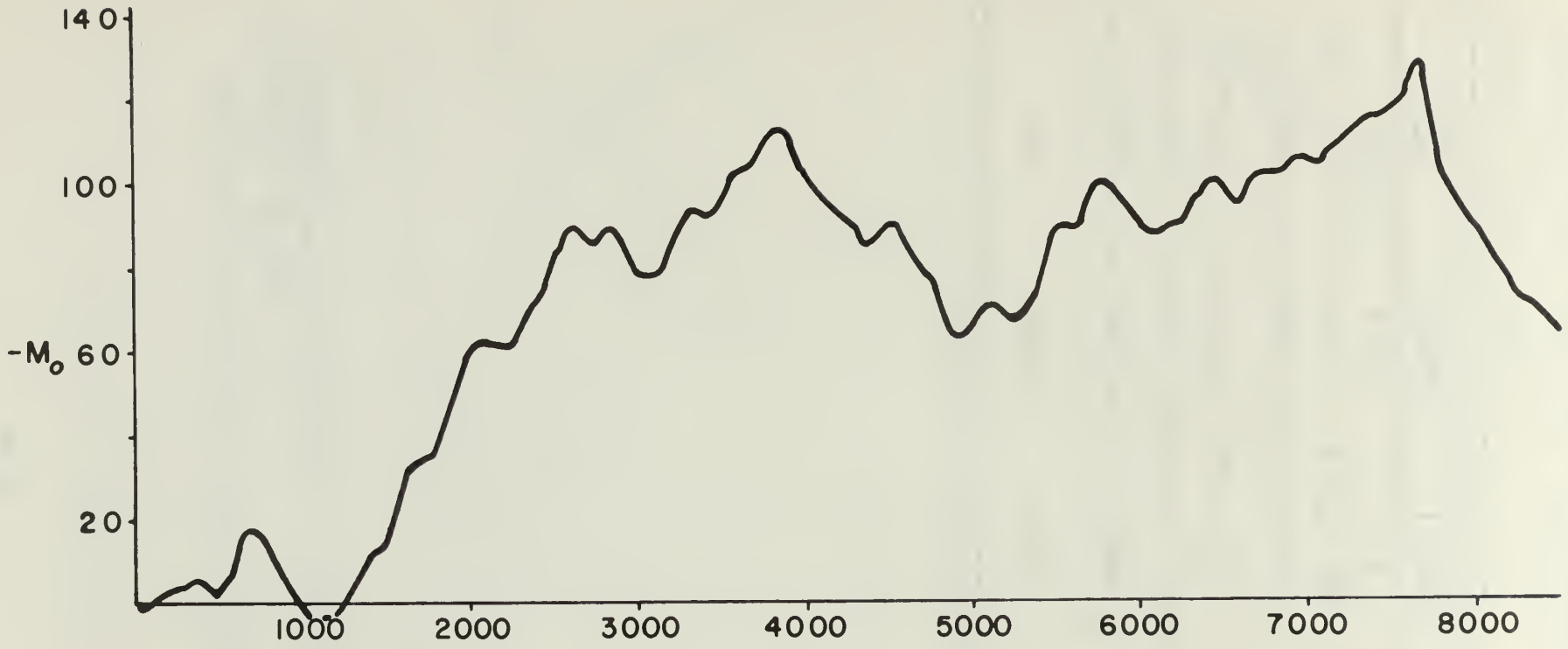

FIG. 7

BENDING MOMENT RESPONSE AT $\phi = 0$ ($\gamma = 1$)

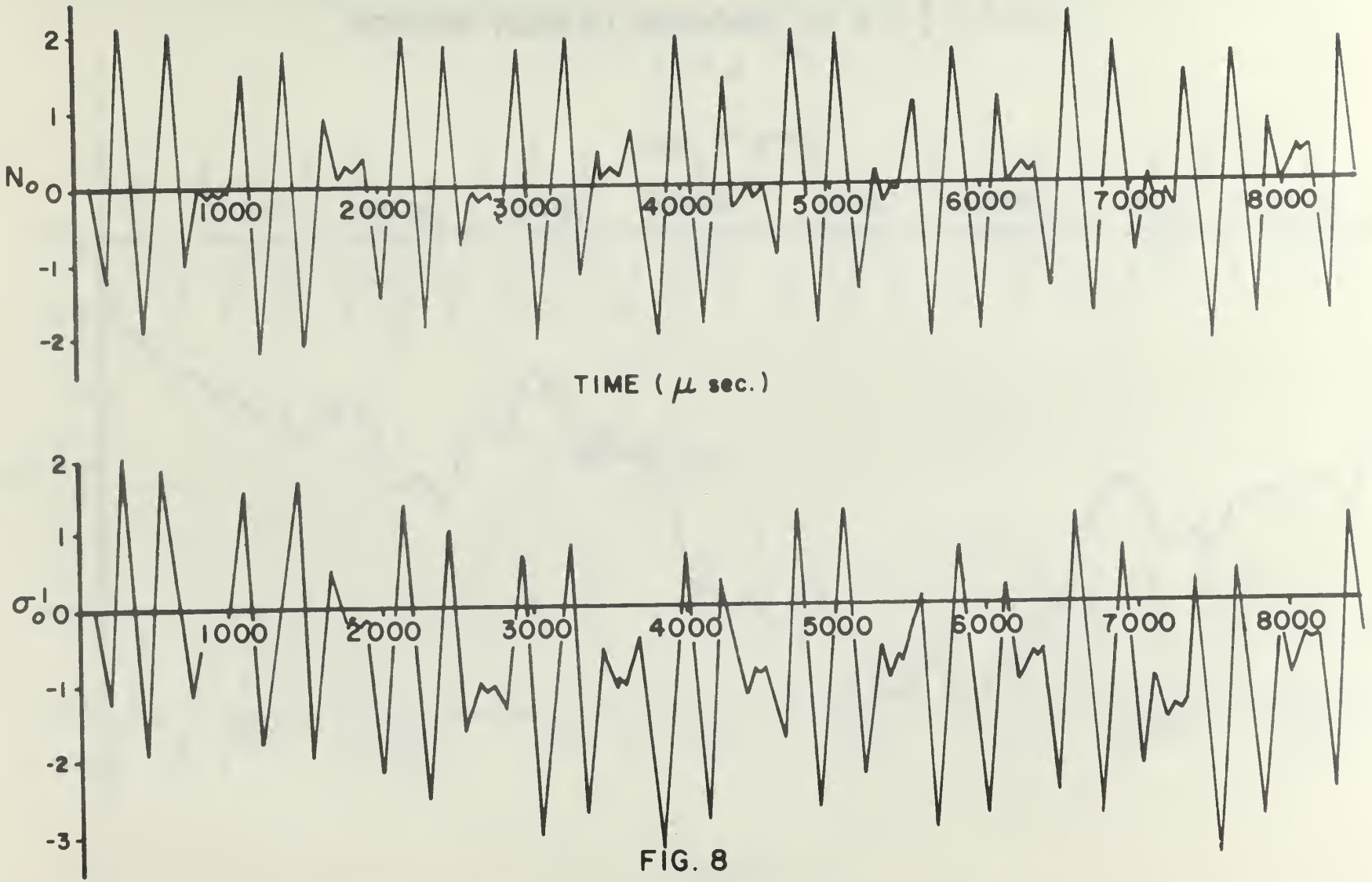

FIG. 8

NORMAL FORCE AND EDGE STRESS AT $\phi = 0$ ($\gamma = 1$)

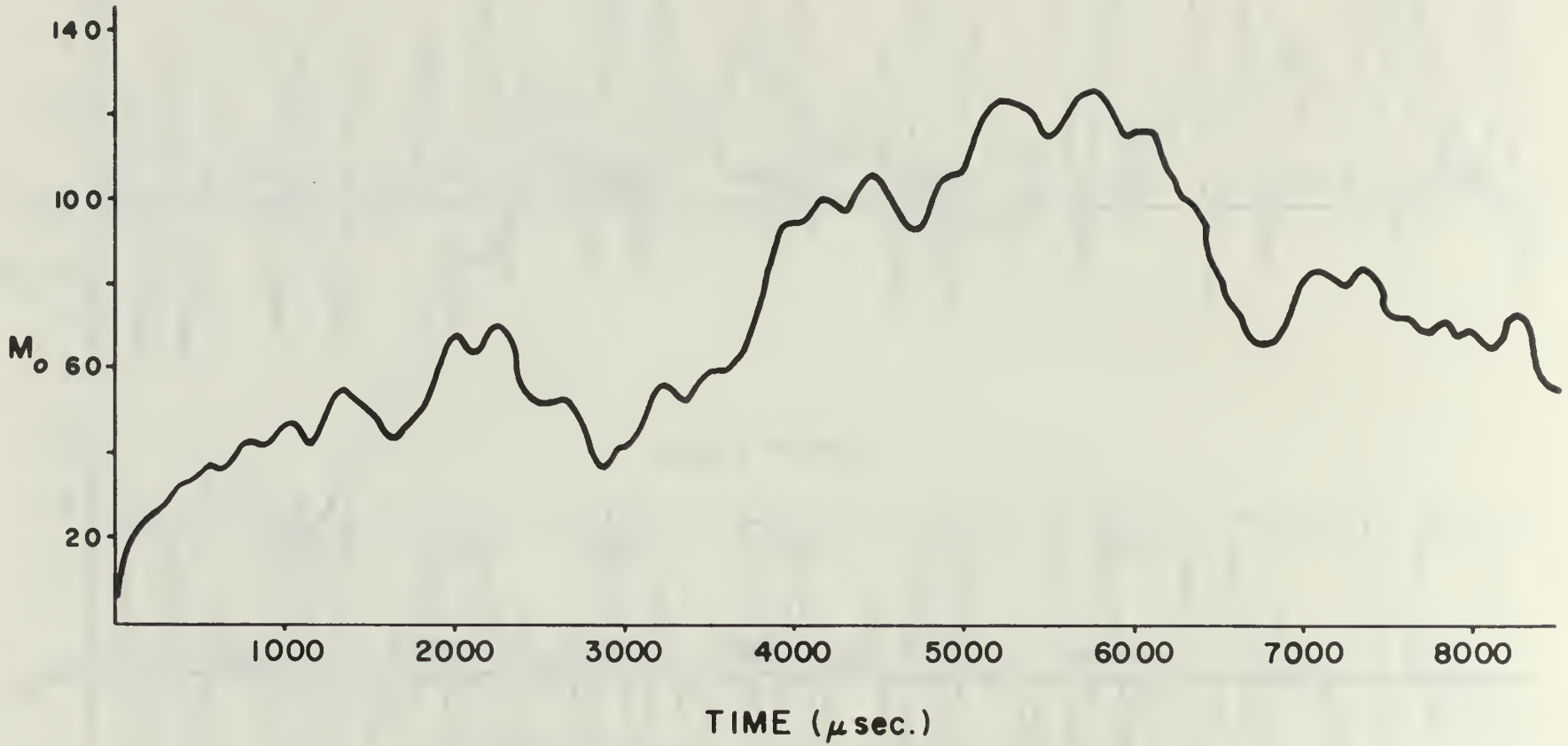

FIG. 9

BENDING MOMENT RESPONSE AT $\phi = \frac{\pi}{2}$ ($\gamma = 1$)

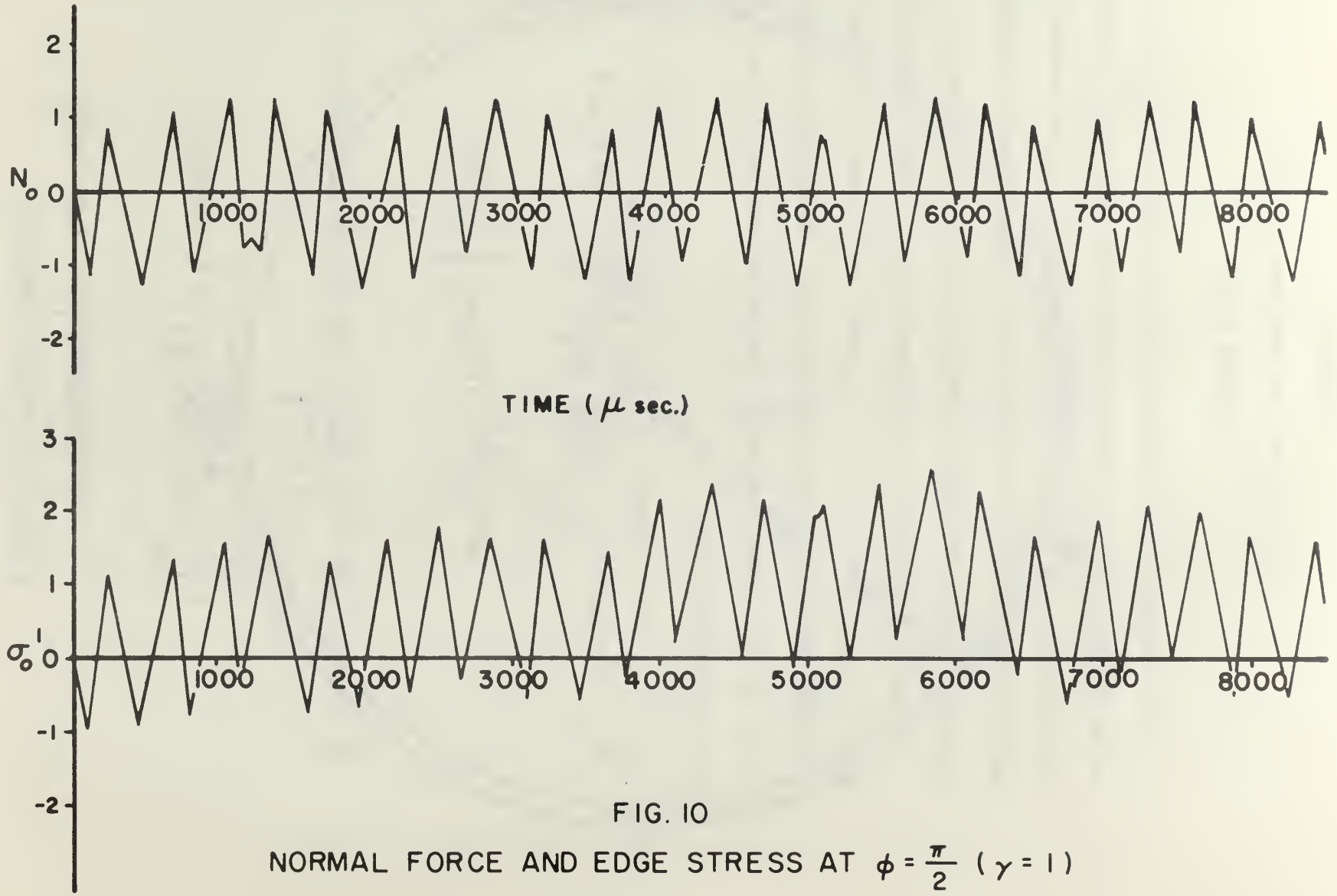

FIG. 10

NORMAL FORCE AND EDGE STRESS AT $\phi = \frac{\pi}{2}$ ($\gamma = 1$)

CHAPTER IV

SOLUTIONS FOR THE IMPULSIVELY LOADED MODIFIED RING

The assumption that the ring's inertia characteristics are variable with regard to tangential vibrations will now be considered. The ring equations must be modified to account for this assumption, and modified solutions analagous to the original ring are obtained in Appendix A for the impulse loading described in Chapter II.

Figure 11 illustrates the assumed inertia forces associated with the ring element, $d\phi$. A simple adjustment of the ring equations will account for this situation. The following expressions for the stress-resultants, derived in Appendix A, are obtained for the modified ring

$$\bar{M}_o = SIN\,\omega_o T + \sum_{n=2,4,\cdots}^{\infty} \frac{-2(-1)^{n/2+1}}{\gamma(\bar{f}_n^2 - \bar{g}_n^2)} \left[\frac{\gamma \bar{f}_n^2 - n^2}{\bar{f}_n} SIN\,\bar{f}_n \omega_o T + \frac{n^2 - \gamma \bar{g}_n^2}{\bar{g}_n} SIN\,\bar{g}_n \omega_o T \right] COS\, n\phi \tag{16}$$

$$\bar{N}_o = -SIN\,\omega_o T + \frac{\pi}{2\sqrt{1+1/\gamma}} SIN \sqrt{1+1/\gamma}\,\omega_o T\, COS\,\phi + \sum_{n=2,4,\cdots}^{\infty} \frac{2(-1)^{n/2+1}}{(n^2-1)(\bar{f}_n^2 - \bar{g}_n^2)} \left[-\bar{f}_n SIN\,\bar{f}_n \omega_o T + \bar{g}_n SIN\,\bar{g}_n \omega_o T \right] COS\, n\phi - \alpha \bar{M}_o \tag{17}$$

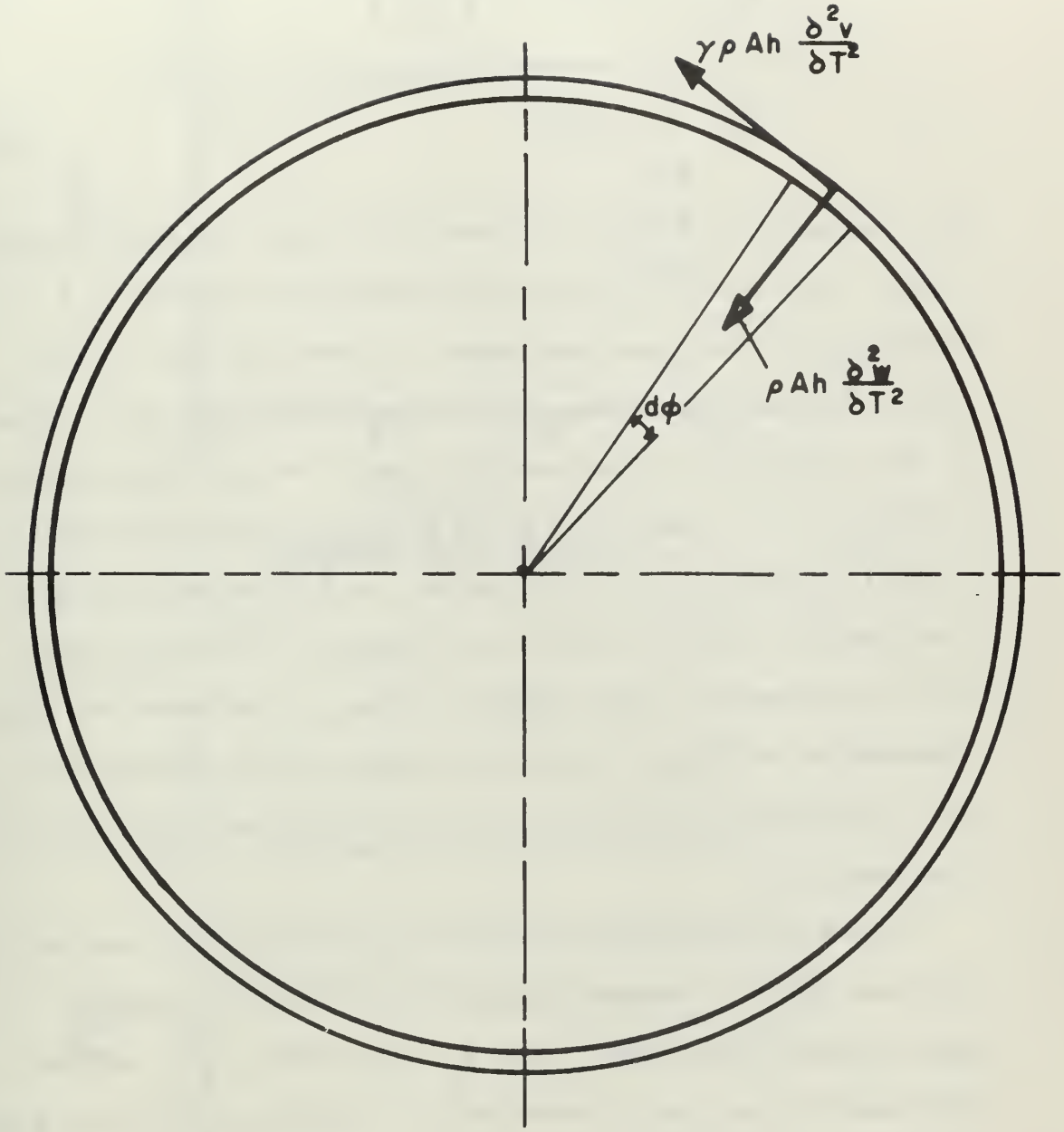

FIG. 11

ASSUMED INERTIA FORCES

To determine the effect of the factor γ on $\bar{M}_o$ and $\bar{N}_o$, consider first the change in the frequency coefficients, $\bar{f}_n$ and $\bar{g}_n$. As determined in Appendix A, these coefficients are

$$\bar{f}_n \doteq n(n^2-1)\sqrt{\frac{\alpha}{n^2+\gamma}} \tag{18}$$

$$\bar{g}_n \doteq \sqrt{\frac{n^2+\gamma}{\gamma}} \tag{19}$$

For this analysis, it will be assumed that γ takes on values between 1 and 4. Therefore, $\bar{f}_n$ will not be significantly affected by γ, especially for the higher mode shapes. However, $\bar{g}_n$ will be very sensitive to a change in γ, as can be seen in Equation (19). Figures 12 and 13 graphically illustrate the error in the modified frequency coefficients as a function of γ. A physical interpretation of the factor γ will verify the above results. As γ increases, a progressively heavier system is seen in the tangential direction, giving rise to a response of lower frequency, $\bar{g}_n \omega_o$. The radial vibrations, characterized by $\bar{f}_n \omega_o$, should not be significantly altered by γ since the density in this direction is always given by the original ring density, ρ.

Values for the modified frequency coefficients have been calculated and listed in Appendix B for the ring defined in Figure 6. Again, it can be seen that $\bar{f}_n << \bar{g}_n$. $\bar{M}_o$ and $\bar{N}_o$, then, will be approximately described by sinusoidals at frequencies $\bar{f}_n \omega_o$ and $\bar{g}_n \omega_o$, respectively.

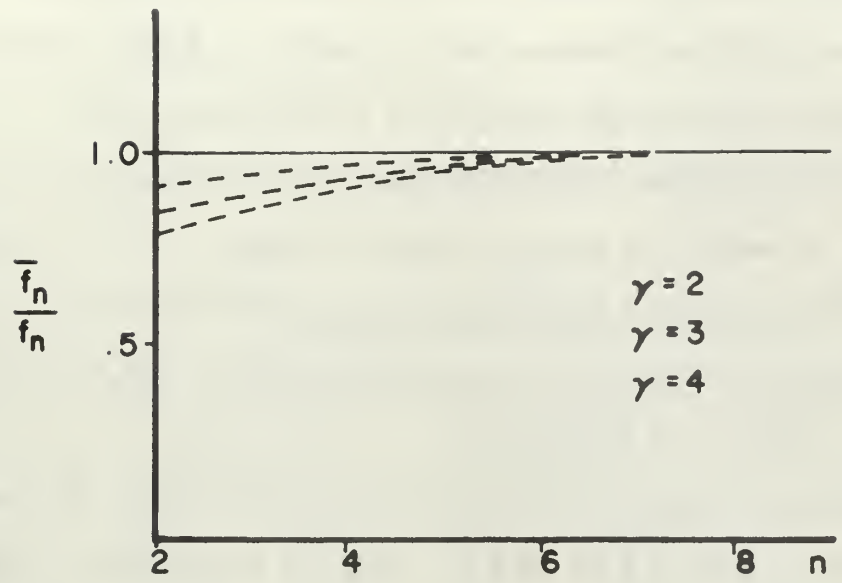

FIG. 12

CHANGE IN $\bar{f}_n$ WITH γ

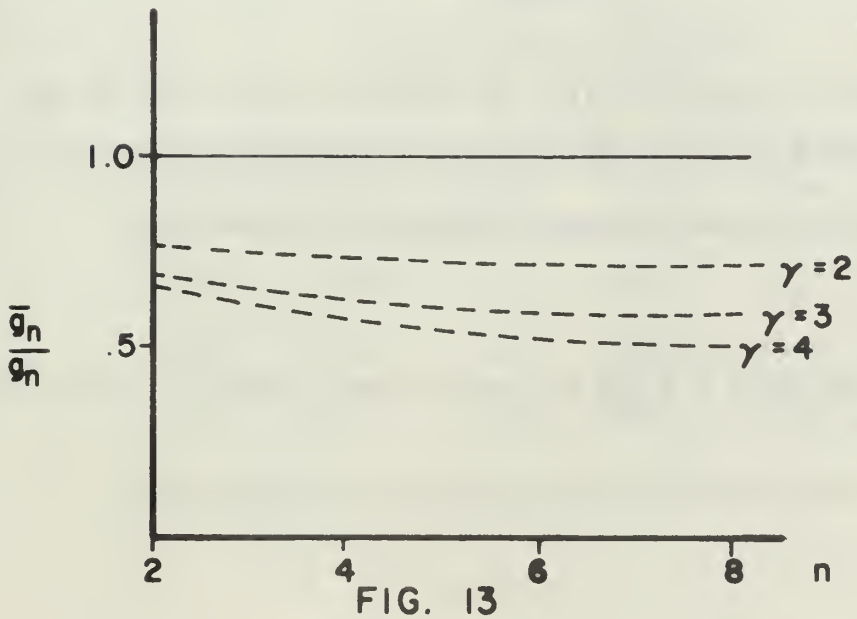

FIG. 13

CHANGE IN $\bar{g}_n$ WITH γ

Examination of the expressions for $\overline{M}_o$ and $\overline{N}_o$ reveals the dominant terms. For the bending moment, Equation (16), the lower frequency sine term will dominate. The magnitude of the coefficient for this term will decrease as the product, $\gamma \overline{g}_n^2$, increases, corresponding to increasing values for γ. Thus, the time response for the bending moment will decrease in magnitude as γ increases. The wave form for the response, however, will not change significantly. Examining Equation (17) in a similar manner, it can be seen that both the wave form and the magnitude of the time response for $\overline{N}_o$ will change as γ increases.

Figures 14 through 19 illustrate the curves for $\overline{M}_o$, $\overline{N}_o$, and $\overline{\sigma}_o'$ for three values of γ at $\phi = 0$. Figures 20 through 22 show $\overline{M}_o$ for $\phi = \frac{\pi}{2}$.* The values obtained for $\overline{M}_o$ and $\overline{N}_o$ at $\phi = \frac{\pi}{4}$ and $\phi = \frac{3\pi}{4}$ were found again to be small compared with other locations on the ring and have been omitted. Also, the curves for $\phi = \pi$ have not been included because of the similarity with the response for $\phi = 0$.

Tables II through IV list the maximum values observed for the solutions of $\overline{M}_o$, $\overline{N}_o$ and $\overline{\sigma}_o'$. The corresponding values for the unmodified ring have also been included for comparison.

*$\overline{N}_o$ and $\overline{\sigma}_o'$ at $\phi = \frac{\pi}{2}$ are not included because of their small magnitudes.

TABLE II

MAXIMUM BENDING MOMENTS

ϕ	$\gamma=1$	$\gamma=2$	$\gamma=3$	$\gamma=4$
0	-129.6	-129.5	-124.9	-117.7
$\frac{\pi}{2}$	125.8	118.3	110.4	103.2
π	-129.6	-129.5	-124.9	-117.7

TABLE III

MAXIMUM NORMAL FORCE (MAGNITUDES)

ϕ	$\gamma=1$	$\gamma=2$	$\gamma=3$	$\gamma=4$
0	2.22	2.38	2.50	2.48
$\frac{\pi}{2}$	1.31	1.48	1.14	1.13
π	2.39	2.43	2.46	2.48

TABLE IV

MAXIMUM OUTER EDGE STRESS

ϕ	$\gamma=1$	$\gamma=2$	$\gamma=3$	$\gamma=4$
0	-3.45	-3.49	-3.28	-3.57
$\frac{\pi}{2}$	2.57	2.38	2.20	2.18
π	-3.27	-3.09	-3.31	-2.98

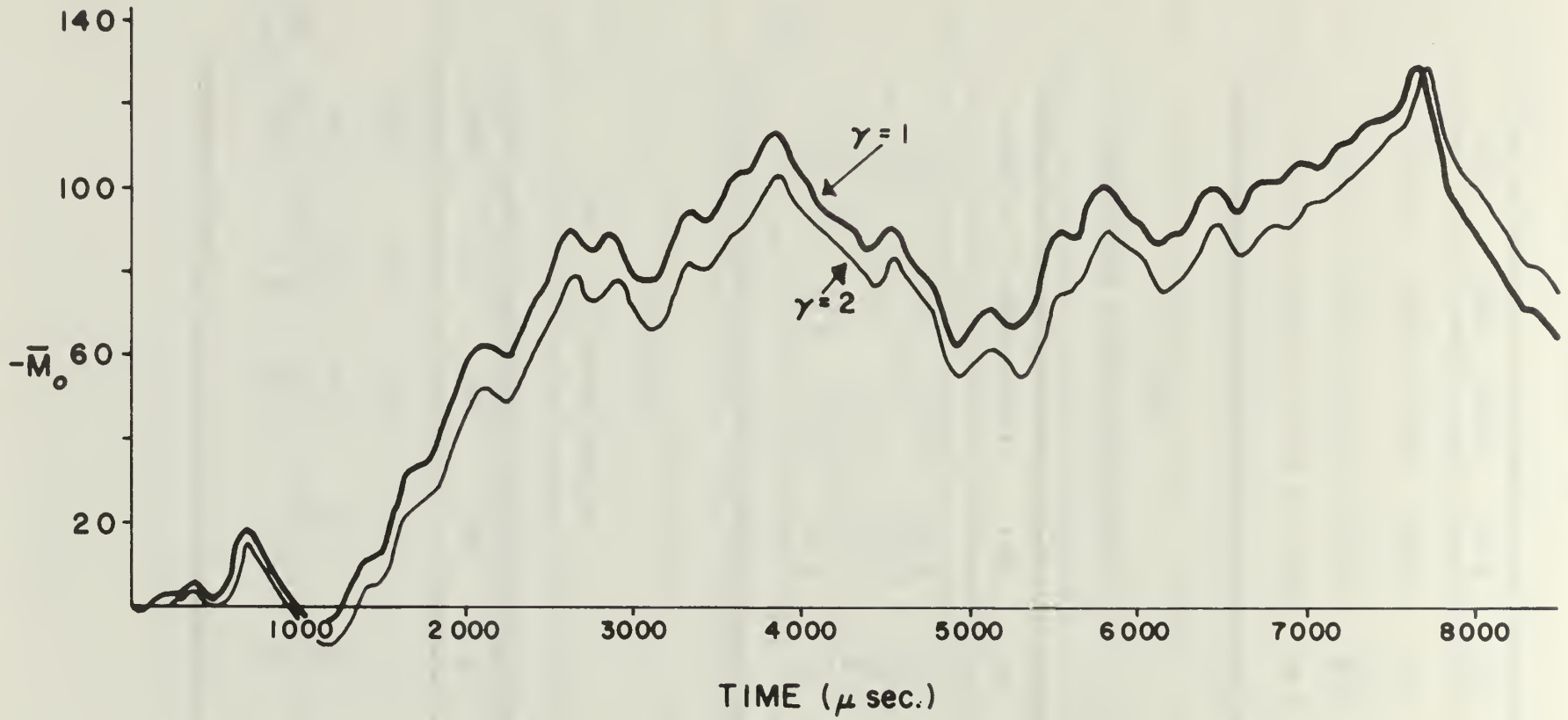

FIG. 14

BENDING MOMENT RESPONSE AT $\phi = 0$ ($\gamma = 2$)

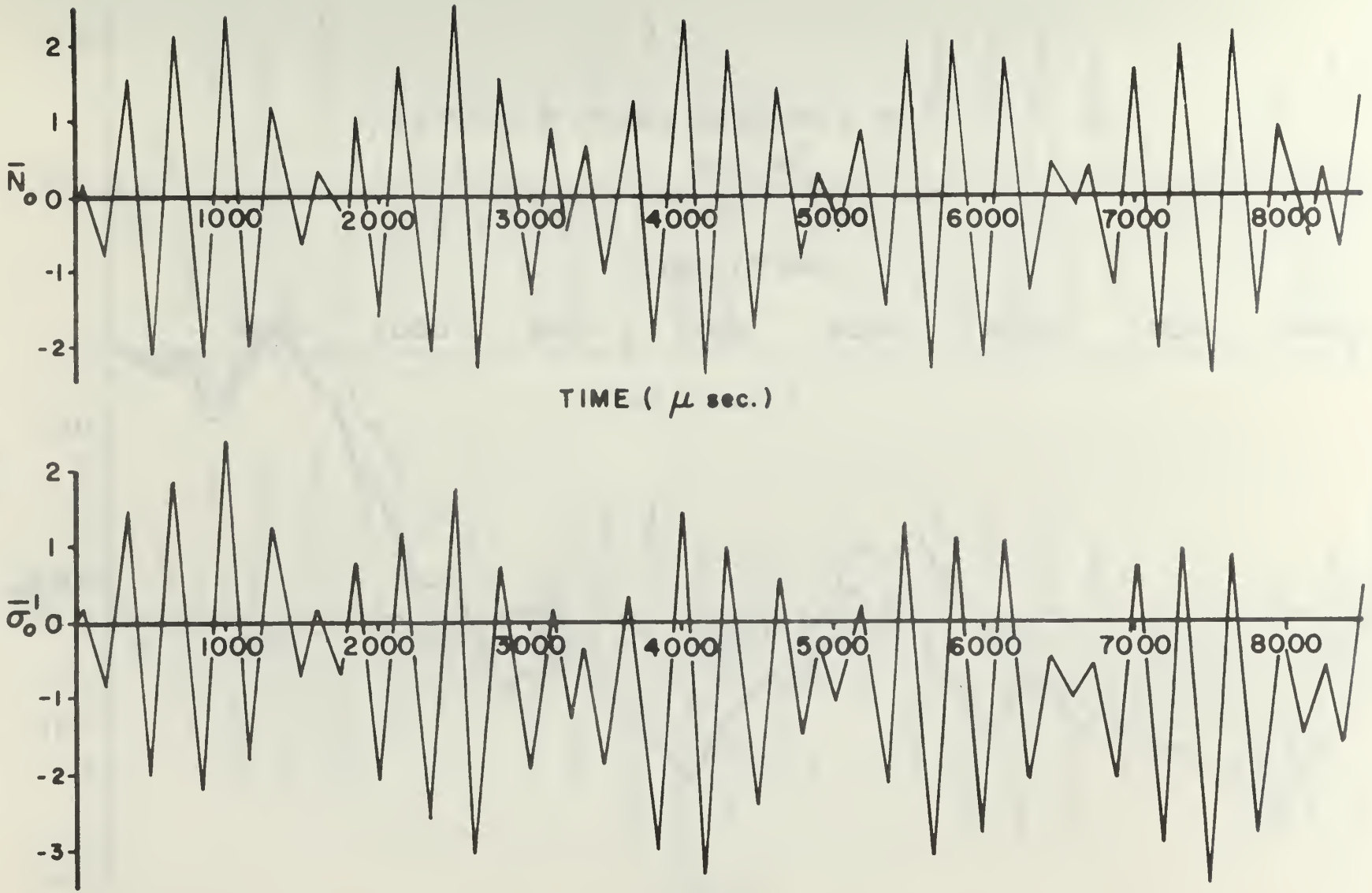

FIG. 15

NORMAL FORCE AND EDGE STRESS AT $\phi = 0$ ($\gamma = 2$)

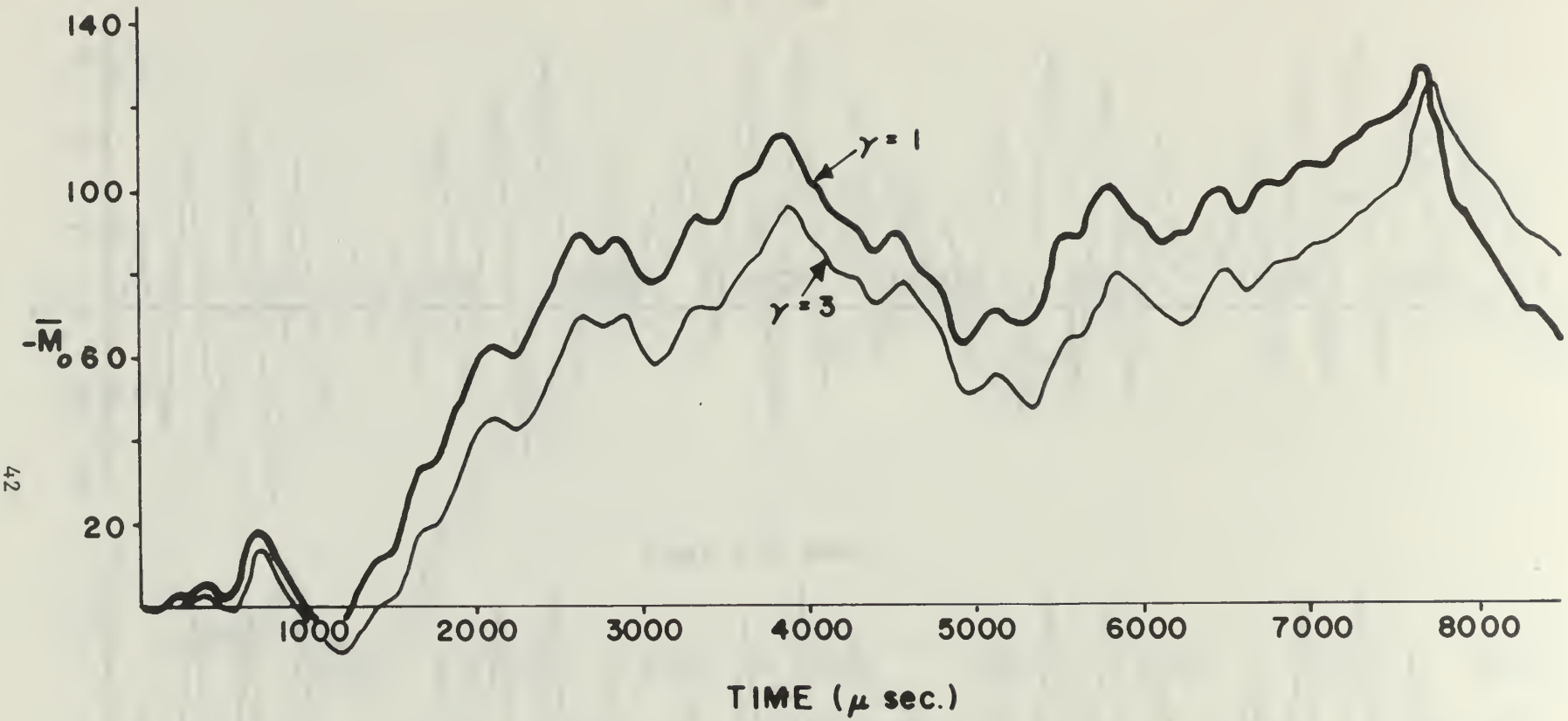

FIG. 16

BENDING MOMENT RESPONSE AT $\phi = 0$ ($\gamma = 3$)

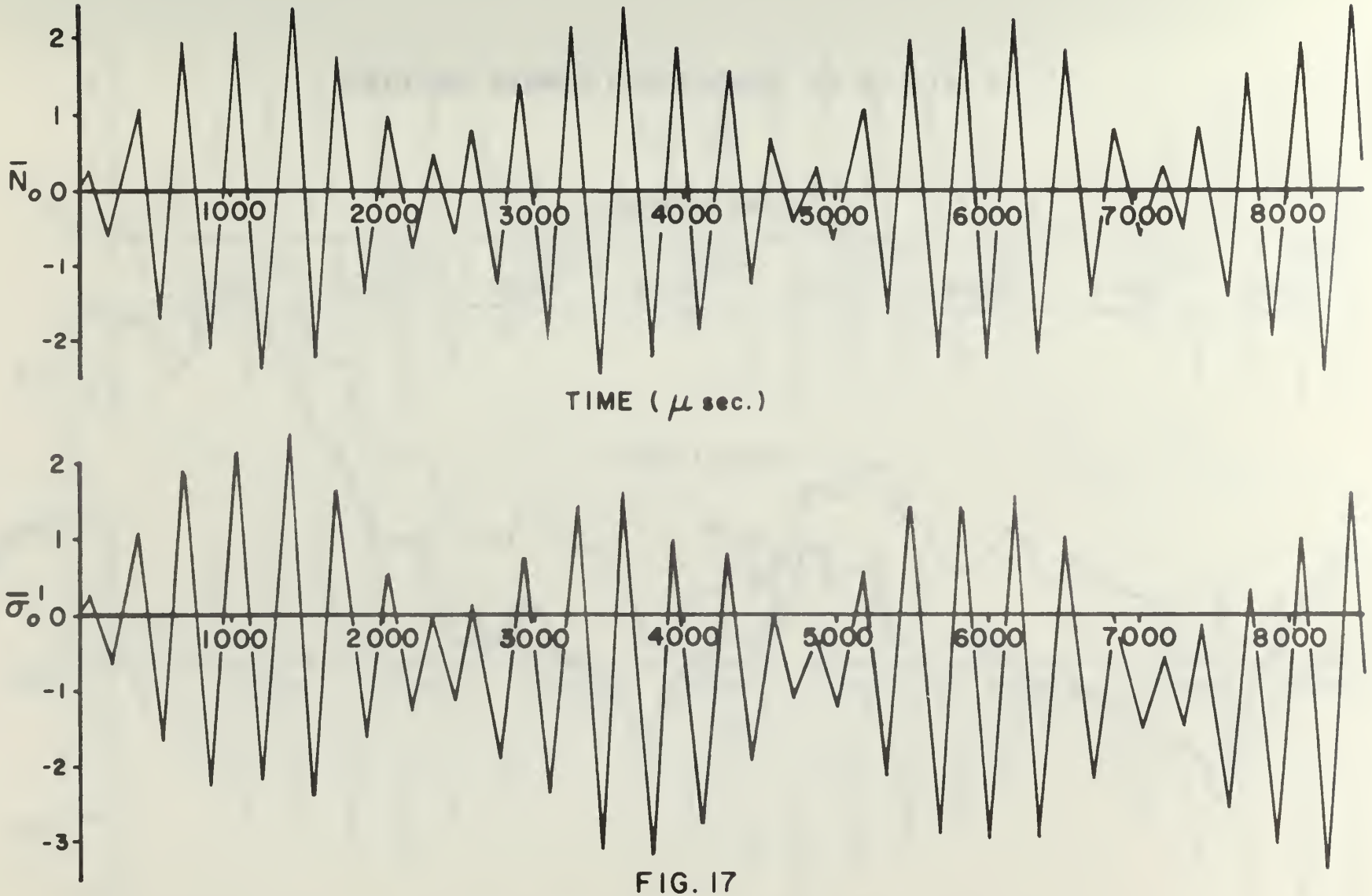

FIG. 17

NORMAL FORCE AND EDGE STRESS AT $\phi = 0$ ($\gamma = 3$)

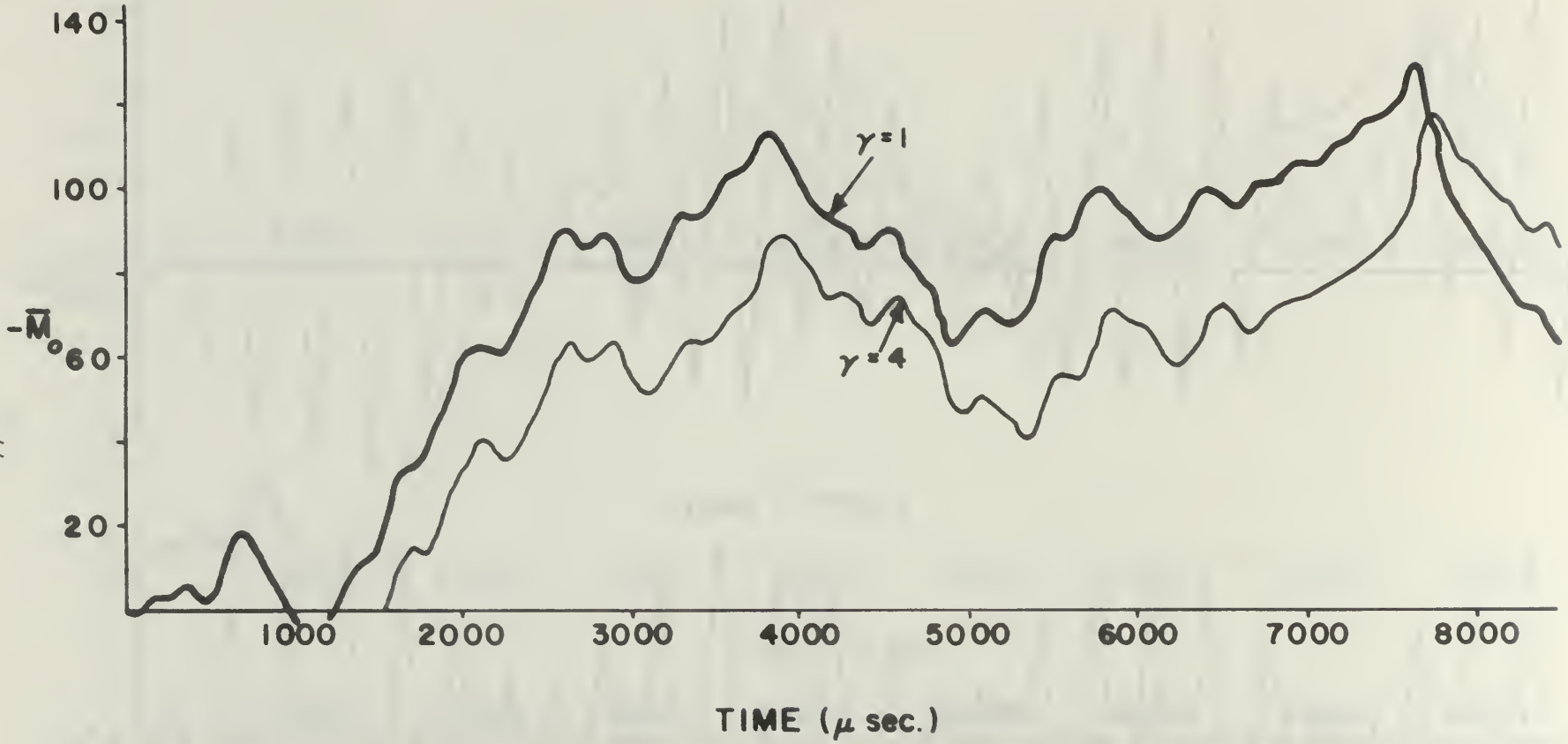

FIG. 18

BENDING MOMENT RESPONSE AT $\phi = 0 (\gamma = 4)$

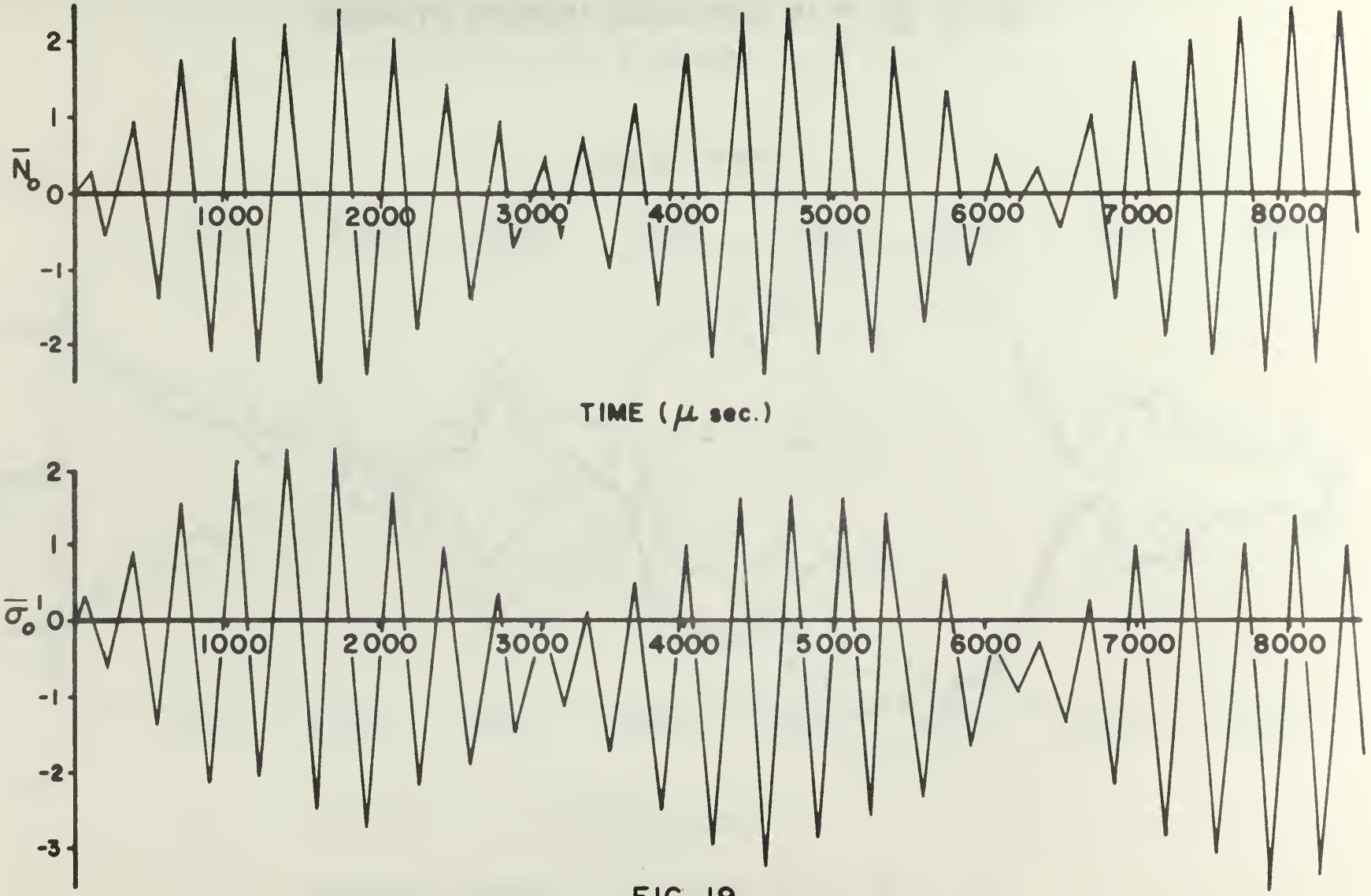

FIG. 19

NORMAL FORCE AND EDGE STRESS AT $\phi = 0$ ($\gamma = 4$)

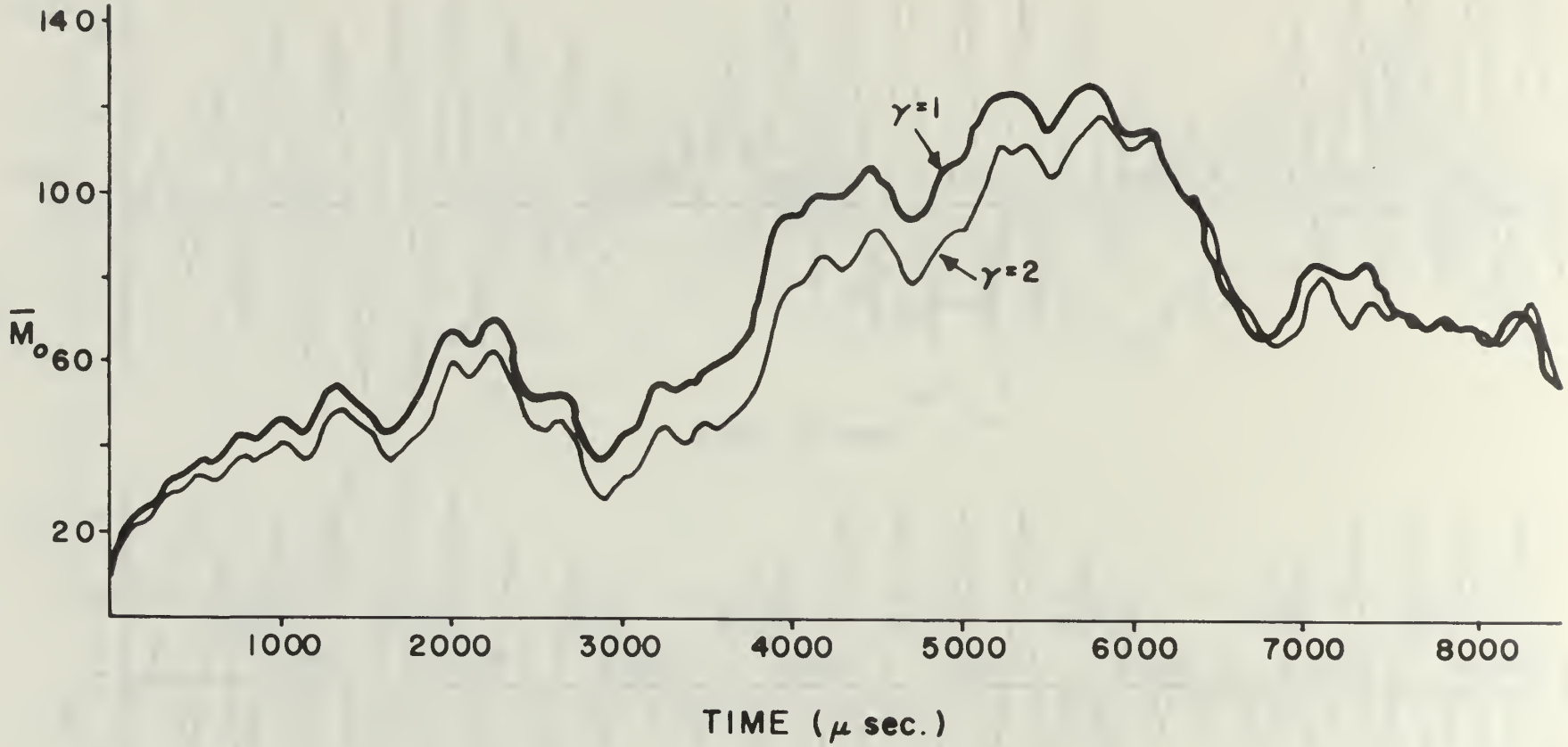

FIG. 20

BENDING MOMENT RESPONSE AT $\phi = \frac{\pi}{2}$ ($\gamma = 2$)

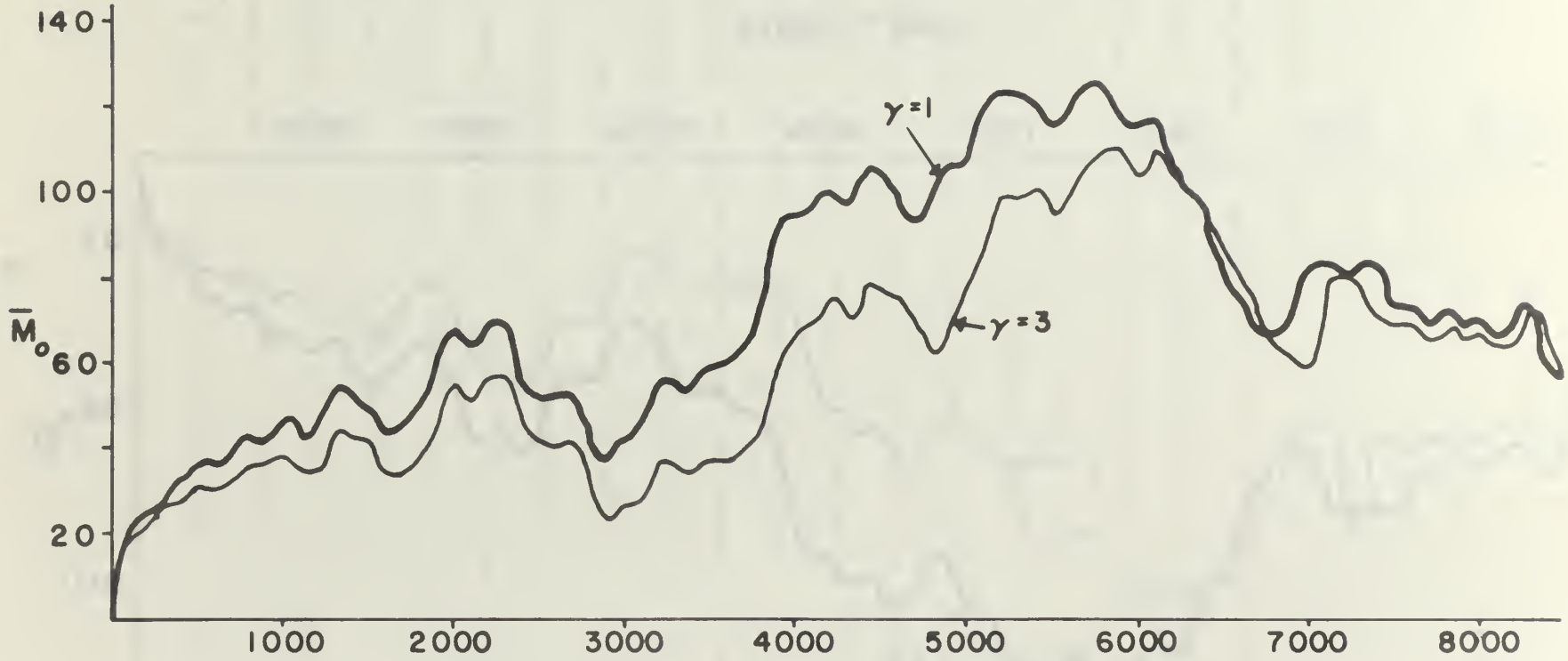

FIG. 21

BENDING MOMENT RESPONSE AT $\phi = \frac{\pi}{2}$ ($\gamma = 3$)

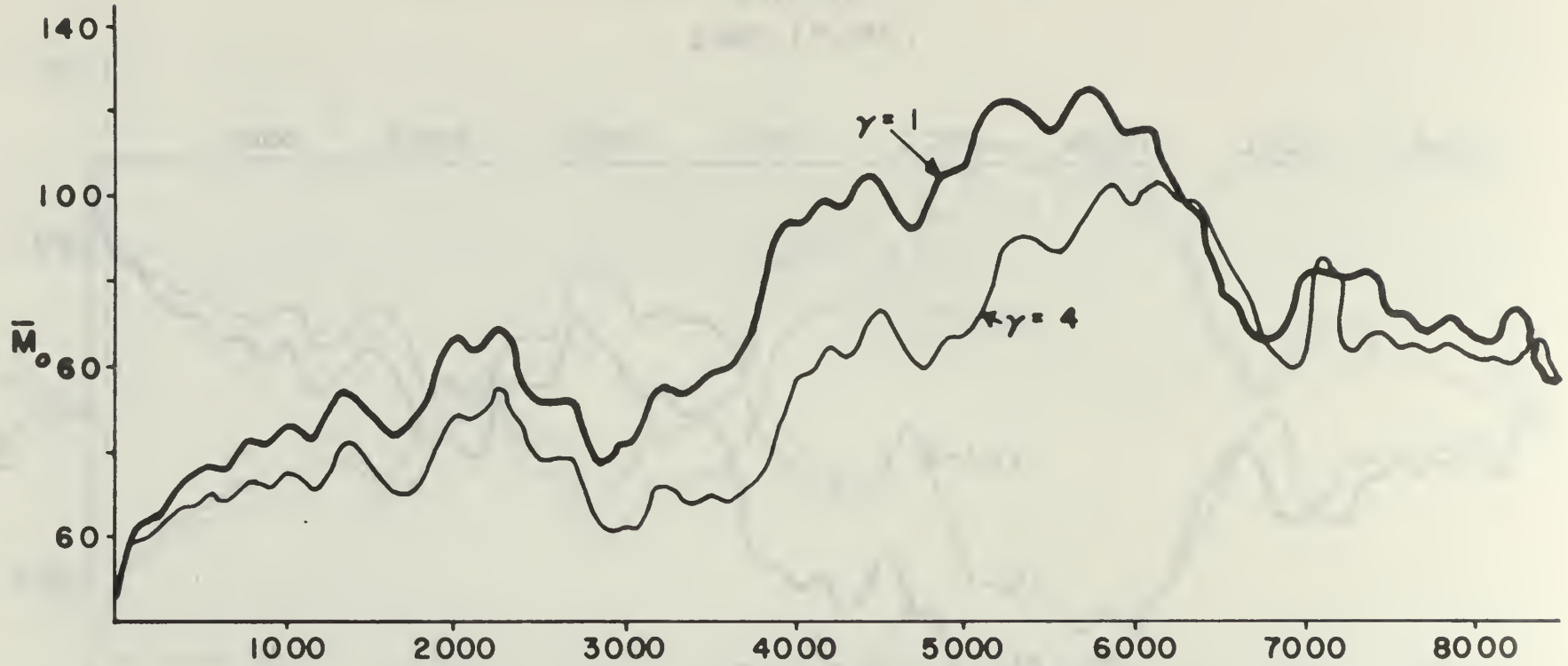

FIG. 22

BENDING MOMENT RESPONSE AT $\phi = \frac{\pi}{2}$ ($\gamma = 4$)

CHAPTER V

CONCLUSIONS

A comparison of the response of the original ring with the results for the modified ring with $\gamma = 2$, 3, and 4 can be made using the data presented in Tables I through IV and the response curves shown in Figures 14 through 22. A study of the time response for the bending moment, M_o and $\overline{M}_o$, reveals that the solutions to the modified ring, in general, range from fair ($\gamma = 2$) to poor ($\gamma = 4$) approximations to the solution for the original ring. Average errors range from 10 per cent for $\gamma = 2$, to about 40 per cent, for $\gamma = 4$. However, the percentage error associated with each modified curve is nearly constant, and the wave form is identical to the unmodified curve. It would appear, then, that the data from a modified solution could be increased by some constant factor to yield a very good approximation over the first quarter cycle.

Based upon the above comparison, the proposed method appears to introduce unacceptable errors into the solution for $\gamma > 2$. However, the actual time response for the bending moment is of little significance in a dynamic analysis, since the maximum value of bending moment is usually the desired result. The maximum bending moments observed for all solutions have been listed in Table II. Based on these values the solutions for the modified ring are very good approximations to the results for the unmodified ring. Errors in the maximum bending moment of about 4 per cent and 8 per cent can be seen for γ values of 3 and 4, with essentially no error observed at $\gamma = 2$.

The effect of a heavier system in the tangential direction is readily observed in an examination of the various normal force response curves. Both the wave forms and the maximum values are affected by a change in the factor γ. As anticipated, the tangential vibrations decrease in frequency as γ increases. This can be seen from the spacing of the beats. Despite the obvious changes in the normal force curves for the modified ring, the maximum peak values, listed in Table III, are not significantly altered as γ changes.

The primary concern of any dynamic analysis is usually the maximum stress that occurs in the ring. Since both the bending moment and the normal force contribute to the stresses, the maximum value will be found on one edge of the ring. The relative importance of each contributor, $\overline{M}_o$ and $\overline{N}_o$, can readily be seen from the stress curves found in Figures 14 through 19. Table IV lists the maximum non-dimensional values found from these curves. The bottom of the ring, $\phi = 0$, is seen to be the critical stress location. A non-dimensional value of -3.45 is the maximum stress calculated from the solution for the original ring. In comparison, the modified ring solutions have values of -3.49, -3.28, and -3.57, all of which are within 5 per cent of the original ring result. Consequently, the assumption of an artificial tangential density has a negligible effect on the ring's maximum dynamic response for the impulsive loading condition considered.

In conclusion, the proposed method for reducing the stability restrictions presented in Chapter I appears to be valid. The same method when applied to the finite difference approach should produce results very similar to those presented here. Thus, because of the assumed artificial tangential inertia, an accurate finite difference solution should be obtained with the computation time reduced by about 30 per cent for $\gamma = 2$, 40 per cent for $\gamma = 3$, and 50 per cent for $\gamma = 4$ from that of the unmodified ring analysis.

REFERENCES

1. Ball, Robert E.; Schjelderup, H. C., "A Feasibility Study of the Numerical Computation of the Inelastic Response of Impulsively Loaded Shells," National Engineering Science Co., Final Report No. P-443-2, June, 1963.
2. Ball, Robert E., "Dynamic Analysis of Rings by Finite Differences," JEM, ASCE, Vol. 93, No. EM1, February, 1967, pp. 1-10.
3. Crandall, Stephen H., Engineering Analysis, McGraw-Hill Book Company, New York, 1956.
4. Flugge, Wilhelm, Stresses in Shells, Springer-Verlag, Berlin, 1960.

APPENDIX A

SOLUTION FOR THE SPECIFIC IMPULSE LOADING

The derivation for the solution to the radial cosine impulse is outlined in this appendix. It should be noted that the development is identical to that of the exact solution when the factor $\gamma = 1$.

Assuming that the density in the tangential direction is larger by a factor γ than that associated with the radial direction, the following modification in the ring equations will result

$$\frac{D}{A}\left(\frac{\partial^2 V}{\partial \phi^2} - \frac{\partial W}{\partial \phi}\right) = \gamma \rho A h \frac{\partial^2 V}{\partial T^2} \tag{A-1}$$

$$\frac{K}{A^3}\left(\frac{\partial^4 W}{\partial \phi^4} + 2\frac{\partial^2 W}{\partial \phi^2} + W\right) - \frac{D}{A}\left(\frac{\partial V}{\partial \phi} - W\right) = -\rho A h \frac{\partial^2 W}{\partial T^2} \tag{A-2}$$

Solutions for W and V were assumed earlier in Equations (11a) and (11b) and are repeated below.

$$\left.\begin{aligned} W(\phi, T) &= \sum_{n=0}^{\infty} A_n(T) \cos n\phi \\ V(\phi, T) &= \sum_{n=1}^{\infty} B_n(T) \sin n\phi \end{aligned}\right\} \tag{A-3}$$

The symmetric and anti-symmetric forms for W and V arise from the symmetry of the impulse and the definition of the V, W coordinate system.

Substituting the assumed solutions into the modified ring equations, Equations (A-1) and (A-2), and setting the two algebraic expressions equal to zero for each value of n lead to

$$Dn(A_n - nB_n) - \gamma A^2 \rho h \frac{\partial^2 B_n}{\partial T^2} = 0 \tag{A-4}$$

$$D(A_n - nB_n) + A_n \frac{K}{A^2}(n^2-1)^2 + A^2 \rho h \frac{\partial^2 A_n}{\partial T^2} = 0 \tag{A-5}$$

for $n = 1, 2, \ldots, \infty$

Harmonic forms are assumed for A_n and B_n

$$\left.\begin{aligned} A_n(T) &= a_n e^{i\omega_n T} \\ B_n(T) &= b_n e^{i\omega_n T} \end{aligned}\right\} \tag{A-6}$$

where a_n and b_n are arbitrary constants. Substitution of these assumed solutions for the time functions into Equations (A-4) and (A-5) yields the following two expressions from which the common time term, $e^{i\omega_n T}$, has been eliminated

$$Dn(a_n - nb_n) + \gamma A^2 \rho h \omega_n^2 b_n = 0 \tag{A-7}$$

$$D(a_n - nb_n) + a_n \frac{K}{A^2}(n^2-1)^2 - A^2 \rho h \omega_n^2 a_n = 0 \tag{A-8}$$

The coefficients a_n and b_n cannot be determined from the above equations since a third unknown, ω_n, is involved. However, they may be expressed in terms of one another and eliminated from both expressions.

From Equation (A-7)

$$a_n = b_n\left[n - \frac{\gamma A^2 \rho h \omega_n^2}{Dn}\right] \tag{A-9}$$

Replacing a_n in Equation (A-8) with the expression above, the constant b_n is common to all terms and may be factored out. A single equation in the unknown ω_n results

$$\frac{\gamma}{n}\left(\frac{\omega_n}{\omega_o}\right)^4 - \left(\frac{\gamma}{n} + \frac{\gamma\alpha(n^2-1)^2}{n} + n\right)\left(\frac{\omega_n}{\omega_o}\right)^2 + n\alpha(n^2-1)^2 = 0 \tag{A-10}$$

where

$$\omega_o = \frac{1}{A}\sqrt{\frac{D}{\rho h}} \qquad\qquad \alpha = \frac{K}{DA^2}$$

The modal frequency ω_n for the time functions A_n and B_n may now be determined. Although four values for ω_n will satisfy Equation (A-10), only two, the positive roots, have physical significance. These roots indicate that each mode of vibration is characterized by two distinct frequencies

$$\left.\begin{aligned} \omega_n &= \bar{f}_n \omega_o \quad * \\ \omega_n &= \bar{g}_n \omega_o \end{aligned}\right\} \tag{A-11}$$

---

* The bars indicate that the frequency coefficients are functions of γ .

where

$$\bar{f}_n = \frac{\left[(n^2+\gamma)+\alpha\gamma(n^2-1)^2 - \sqrt{(n^2+\gamma)^2 - 2\alpha(n^2-1)^2(\gamma n^2-\gamma^2)+\gamma^2\alpha^2(n^2-1)^4}\right]^{1/2}}{\sqrt{2\gamma}}$$

$$\bar{g}_n = \frac{\left[(n^2+\gamma)+\alpha\gamma(n^2-1)^2 + \sqrt{(n^2+\gamma)^2 - 2\alpha(n^2-1)^2(\gamma n^2-\gamma^2)+\gamma^2\alpha^2(n^2-1)^4}\right]^{1/2}}{\sqrt{2\gamma}} \qquad \text{(A-12)}$$

The frequency coefficients $\bar{f}_n$ and $\bar{g}_n$ may be simplified in light of the thin ring assumption. For small values of α *, these coefficients are approximated by

$$\left.\begin{aligned} \bar{f}_n &\doteq n(n^2-1)\sqrt{\frac{\alpha}{n^2+\gamma}} \\ \bar{g}_n &\doteq \sqrt{\frac{n^2+\gamma}{\gamma}} \end{aligned}\right\} \qquad \text{(A-13)}$$

The initial values for the time functions must now be determined in order to solve for the constants a_n and b_n. At time $T = 0$, the expressions for the displacements and velocities are simple Fourier series expansions in the single variable Φ. The Fourier coefficients for these series may be evaluated to yield the following initial conditions for $A_n(T)$ and $B_n(T)$

$$A_n(0) = 0 \qquad\qquad n = 0, 1, 2, \ldots$$

*For the problem considered, $\alpha = 3.54 \times 10^{-5}$.

$$\frac{\partial A_0}{\partial T}(0) = \frac{V_0}{\pi}$$

$$\frac{\partial A_1}{\partial T}(0) = -\frac{V_0}{4}$$

$$\frac{\partial A_n}{\partial T}(0) = \frac{2V_0(-1)^{n/2+1}}{(n^2-1)\pi} \qquad n = 2, 4, 6, \ldots$$

$$= 0 \qquad n = 3, 5, 7, \ldots$$

$$B_n(0) = 0 \qquad n = 1, 2, 3, \ldots$$

$$\frac{\partial B_1}{\partial T}(0) = \frac{V_0}{4}$$

$$\frac{\partial B_n}{\partial T}(0) = 0 \qquad n = 2, 3, 4, \ldots$$

(A-14)

The time functions may now be determined from the above initial values. For the cases n = 0 and n = 1, a simple substitution into the modified ring equations yields

$$A_o(T) = \frac{V_o}{\pi \omega_o} \sin \omega_o T \tag{A-15}$$

and

$$\left.\begin{aligned} A_1(T) &= \frac{-V_o}{4\sqrt{1+\frac{1}{\gamma}}\,\omega_o} \sin \sqrt{1+\frac{1}{\gamma}}\,\omega_o T \\ B_1(T) &= \frac{V_o}{4\sqrt{1+\frac{1}{\gamma}}\,\omega_o} \sin \sqrt{1+\frac{1}{\gamma}}\,\omega_o T \end{aligned}\right\} \tag{A-16}$$

The solution for the higher mode shapes, n > 1, requires further explanation. Recalling that the modal frequency ω_n was characterized by four distinct roots, there are four separate solutions for A_n and B_n which satisfy the ring equations. The sums of these solutions are also solutions. Therefore, the general time functions for n > 1 are

$$A_n(T) = \bar{a}_{n1} e^{i\bar{f}_n \omega_o T} + \bar{a}_{n2} e^{-i\bar{f}_n \omega_o T} + \bar{a}_{n3} e^{i\bar{g}_n \omega_o T} + \bar{a}_{n4} e^{-i\bar{g}_n \omega_o T} \tag{A-17}$$

$$B_n(T) = \bar{b}_{n1} e^{i\bar{f}_n \omega_o T} + \bar{b}_{n2} e^{-i\bar{f}_n \omega_o T} + \bar{b}_{n3} e^{i\bar{g}_n \omega_o T} + b_{n4} e^{-i\bar{g}_n \omega_o T}$$

Although eight constants appear in the above equations, only four are independent. As determined earlier in Equation (A-9), the $\bar{b}$ constants may be replaced with expressions involving the $\bar{a}$ constants. Applying Equations (A-13), these relationships are

$$\left.\begin{aligned} \bar{b}_{n1} &= \bar{a}_{n1}\left[\frac{n}{n^2-\gamma\bar{f}_n^2}\right] \quad ; \quad \bar{b}_{n2} = \bar{a}_{n2}\left[\frac{n}{n^2-\gamma\bar{f}_n^2}\right] \\ \bar{b}_{n3} &= \bar{a}_{n3}\left[\frac{n}{n^2-\gamma\bar{g}_n^2}\right] \quad ; \quad \bar{b}_{n4} = \bar{a}_{n4}\left[\frac{n}{n^2-\gamma\bar{g}_n^2}\right] \end{aligned}\right\} \quad \text{(A-18)}$$

Substituting Equation (A-18) into Equation (A-17), the expressions for $A_n(T)$ and $B_n(T)$ contain four unknown constants to which four initial conditions may be imposed.

To apply the initial conditions, Equations (A-14), the time functions must be expressed in terms of sines and cosines. Making the appropriate expansions for the exponentials and regrouping the $\bar{a}$ constants into new constants, $\bar{\bar{a}}$, Equations (A-17) become

$$\left.\begin{aligned} A_n(T) &= \bar{\bar{a}}_{n1}\cos\bar{f}_n\omega_o T + \bar{\bar{a}}_{n2}\,SIN\,\bar{f}_n\omega_o T \\ &\quad + \bar{\bar{a}}_{n3}\cos\bar{g}_n\omega_o T + \bar{\bar{a}}_{n4}\,SIN\,\bar{g}_n\omega_o T \\ B_n(T) &= \frac{n}{n^2-\gamma\bar{f}_n^2}\left[\bar{\bar{a}}_{n1}\cos\bar{f}_n\omega_o T + \bar{\bar{a}}_{n2}\,SIN\,\bar{f}_n\omega_o T\right] \\ &\quad + \frac{n}{n^2-\gamma\bar{g}_n^2}\left[\bar{\bar{a}}_{n3}\cos\bar{g}_n\omega_o T + \bar{\bar{a}}_{n4}\,SIN\,\bar{g}_n\omega_o T\right] \end{aligned}\right\} \quad \text{(A-19)}$$

A solution may now be determined for the $\bar{\bar{a}}$ constants. Applying the initial conditions, the cosine terms must vanish. Thus,

$$\bar{\bar{a}}_{n1} = \bar{\bar{a}}_{n3} = \bar{\bar{b}}_{n1} = \bar{\bar{b}}_{n3} = 0 \quad \text{(A-20)}$$

The coefficients for the sine terms are given by the following expressions

$$\bar{\bar{a}}_{n2} = \frac{2V_o(-1)^{n/2+1}(\gamma\bar{f}_n^2 - n^2)}{\gamma\omega_o\pi(n^2-1)(\bar{f}_n^2-\bar{g}_n^2)\bar{f}_n}$$

$$\bar{\bar{a}}_{n4} = \frac{2V_o(-1)^{n/2+1}(n^2-\gamma\bar{g}_n^2)}{\gamma\omega_o\pi(n^2-1)(\bar{f}_n^2-\bar{g}_n^2)\bar{g}_n}$$

$n = 2, 4, 6, ..$ (A-21)

$$\bar{\bar{a}}_{n2} = \bar{\bar{a}}_{n4} = 0$$

$n = 3, 5, 7, ..$ (A-22)

and hence

$$\bar{\bar{b}}_{n2} = \frac{-2V_o(-1)^{n/2+1}\, n}{\gamma\omega_o\pi(n^2-1)(\bar{f}_n^2-\bar{g}_n^2)f_n}$$

$$\bar{\bar{b}}_{n4} = \frac{2V_o(-1)^{n/2+1}\, n}{\gamma\omega_o\pi(n^2-1)(\bar{f}_n^2-\bar{g}_n^2)\bar{g}_n}$$

$n = 2, 4, 6 ...$ (A-23)

$$\bar{\bar{b}}_{n2} = \bar{\bar{b}}_{n4} = 0$$

$n = 3, 5, 7, ..$ (A-24)

The time functions may now be written directly as

$$A_n(T) = \frac{2V_o(-1)^{n/2+1}}{\gamma\omega_o\pi(n^2-1)(\bar{f}_n^2-\bar{g}_n^2)}\left[\frac{\gamma\bar{f}_n^2-n^2}{\bar{f}_n}\,SIN\,\bar{f}_n\omega_o T + \frac{n^2-\gamma\bar{g}_n^2}{\bar{g}_n}\,SIN\,\bar{g}_n\omega_o T\right]$$

$$B_n(T) = \frac{2V_o(-1)^{n/2+1}}{\gamma\omega_o\pi(n^2-1)(\bar{f}_n^2-\bar{g}_n^2)}\left[-\frac{n}{\bar{f}_n}\,SIN\,\bar{f}_n\omega_o T + \frac{n}{\bar{g}_n}\,SIN\,\bar{g}_n\omega_o T\right]$$

even modes ≥ 2 (A-25)

$$A_n(T) = B_n(T) = 0$$

odd modes ≥ 3 (A-26)

These expressions may be substituted into Equation (A-3) to obtain the middle surface displacements, W and V, as functions of time and ring position. As determined earlier in Chapter II, Equations (4)

and (5), the stress-resultants M and N are given in terms of the displacements W and V by

$$\left.\begin{aligned} N &= \frac{D}{A}\left(\frac{\partial V}{\partial \phi} - W\right) - \frac{K}{A^3}\left(\frac{\partial^2 W}{\partial \phi^2} + W\right) \\ M &= -\frac{K}{A^2}\left(\frac{\partial^2 W}{\partial \phi^2} + W\right) \end{aligned}\right\} \quad \text{(A-27)}$$

Thus, the solutions for W, V, M, and N due to the radial cosine impulse become

$$W\frac{\omega_o \pi}{V_o} = \sin \omega_o T - \frac{\pi}{4\sqrt{1+1/\gamma}} \sin\sqrt{1+1/\gamma}\,\omega_o T \cos\phi + \sum_{n=2,4,\cdots}^{\infty} \frac{2(-1)^{n/2+1}}{\gamma(n^2-1)(\bar{f}_n^2 - \bar{g}_n^2)}\left[\frac{\gamma \bar{f}_n^2 - n^2}{\bar{f}_n} \sin \bar{f}_n \omega_o T + \frac{n^2 - \gamma \bar{g}_n^2}{\bar{g}_n} \sin \bar{g}_n \omega_o T\right] \cos n\phi \quad \text{(A-28)}$$

$$V\frac{\omega_o \pi}{V_o} = \frac{\pi}{4\sqrt{1+1/\gamma}} \sin\sqrt{1+1/\gamma}\,\omega_o T \sin\phi + \sum_{n=2,4,\cdots}^{\infty} \frac{2(-1)^{n/2+1}}{\gamma(n^2-1)(\bar{f}_n^2 - \bar{g}_n^2)}\left[-\frac{n}{\bar{f}_n} \sin \bar{f}_n \omega_o T + \frac{n}{\bar{g}_n} \sin \bar{g}_n \omega_o T\right] \sin n\phi \quad \text{(A-29)}$$

and

$$\bar{M}_o = -M \frac{A^2 \pi \omega_o}{K V_o}$$

$$= \sin \omega_o T + \sum_{n=2,4,\ldots}^{\infty} \frac{-2(-1)^{n/2+1}}{\gamma(\bar{f}_n^2 - \bar{g}_n^2)} \left[\frac{\gamma \bar{f}_n^2 - n^2}{\bar{f}_n} \sin \bar{f}_n \omega_o T \right.$$

$$\left. + \frac{n^2 - \gamma \bar{g}_n^2}{\bar{g}_n} \sin \bar{g}_n \omega_o T \right] \cos n\phi \qquad \text{(A-30)}$$

$$\bar{N}_o = N \frac{A \pi \omega_o}{D V_o} = -\sin \omega_o T + \frac{\pi}{2\sqrt{1+1/\gamma}} \sin \sqrt{1+1/\gamma}\, \omega_o T \cos \phi$$

$$+ \sum_{n=2,4,\ldots}^{\infty} \frac{2(-1)^{n/2+1}}{(n^2-1)(\bar{f}_n^2 - \bar{g}_n^2)} \left[-\bar{f}_n \sin \bar{f}_n \omega_o T \right.$$

$$\left. + \bar{g}_n \sin \bar{g}_n \omega_o T \right] \cos n\phi - \alpha \bar{M}_o \qquad \text{(A-31)}$$

APPENDIX B

CALCULATED FREQUENCY COEFFICIENTS

TABLE V

FREQUENCY COEFFICIENTS ($\gamma = 1$)

n	f_n	g_n
2	0.016	2.236
4	0.088	4.123
6	0.208	6.082
8	0.376	8.062
10	0.592	10.050
12	0.857	12.041
14	1.169	14.036
16	1.530	16.031

TABLE VI

FREQUENCY COEFFICIENTS ($\gamma = 2$)

n	$\bar{f}_n$	$\bar{g}_n$
2	0.015	1.732
4	0.085	3.000
6	0.205	4.359
8	0.373	5.745
10	0.589	7.141
12	0.854	8.544
14	1.167	9.950
16	1.528	11.358

TABLE VII

FREQUENCY COEFFICIENTS ($\gamma = 3$)

n	$\bar{f}_n$	$\bar{g}_n$
2	0.014	1.528
4	0.083	2.517
6	0.202	3.606
8	0.370	4.726
10	0.587	5.859
12	0.851	7.000
14	1.163	8.145
16	1.524	9.291

TABLE VII

FREQUENCY COEFFICIENTS ($\gamma = 4$)

n	$\bar{f}_n$	$\bar{g}_n$
2	0.013	1.414
4	0.081	2.236
6	0.199	3.162
8	0.367	4.123
10	0.583	5.099
12	0.848	6.082
14	1.161	7.071
16	1.521	8.062

INITIAL DISTRIBUTION LIST

		No. Copies
1.	Defense Documentation Center Cameron Station Alexandria, Virginia	20
2.	Library Naval Postgraduate School, Monterey, California	2
3.	Commander, Naval Air Systems Command Navy Department Washington, D. C. 20360	1
4.	Professor Robert E. Ball Department of Aeronautics Naval Postgraduate School, Monterey, California	1
5.	Chairman, Department of Aeronautics Naval Postgraduate School, Monterey, California	1
6.	Professor A. E. Fuhs Department of Aeronautics Naval Postgraduate School, Monterey, California	1
7.	Ensign Harold W. Hickman, Jr. 1077 Second Avenue Chula Vista, California 92011	1
8.	Professor L. V. Schmidt Department of Aeronautics Naval Postgraduate School, Monterey, California	1
9.	Superintendent Naval Academy Annapolis, Maryland	1
10.	Head, Department of Engineering Naval Academy Annapolis, Maryland	1
11.	Dr. E. S. Lamar (Code 03C) Chief Scientist Naval Air Systems Command Navy Department Washington, D. C.	1

12. Dr. R. S. Burington — 1
Chief Mathematician
Naval Air Systems Command
Navy Department
Washington, D. C.

13. Commander — 1
Naval Ordnance Systems Command
Navy Department
Washington, D. C.

14. Office of Naval Research — 1
Navy Department
Washington, D. C.

15. Mr. G. L. Desmond — 1
Aerodynamics and Structures Admin. (Code 320)
Research and Technology
Naval Air Systems Command
Navy Department
Washington, D. C.

16. Office of Naval Research — 1
Mathematical Sciences Division, Code 430
Navy Department
Washington, D. C.

17. Office of Naval Research — 1
Air Programs Office
Navy Department
Washington, D. C.

DOCUMENT CONTROL DATA - R&D

(Security classification of title, body of abstract and indexing annotation must be entered when the overall report is classified)

1. ORIGINATING ACTIVITY *(Corporate author)*
Naval Postgraduate School
Monterey, California 93940

2a. REPORT SECURITY CLASSIFICATION
Unclassified

2b GROUP

3. REPORT TITLE

A STUDY TO DETERMINE THE EFFECT OF ARTIFICIAL TANGENTIAL INERTIA ON THE DYNAMIC RESPONSE OF ELASTIC RINGS

4. DESCRIPTIVE NOTES *(Type of report and inclusive dates)*
Masters Thesis, 1967-1968

5. AUTHOR(S) *(Last name, first name, initial)*

Hickman, Harold W., Jr., Ens., USN

6. REPORT DATE	7a. TOTAL NO. OF PAGES	7b. NO. OF REFS
March 1968	65	4

8a. CONTRACT OR GRANT NO.	9a. ORIGINATOR'S REPORT NUMBER(S)
b. PROJECT NO.	
c.	9b. OTHER REPORT NO(S) *(Any other numbers that may be assigned this report)*
d.	

10. AVAILABILITY/LIMITATION NOTICES

[redacted]

11. SUPPLEMENTARY NOTES	12. SPONSORING MILITARY ACTIVITY
	Superintendent Naval Postgraduate School Monterey, California 93940

13 ABSTRACT

The elastic transient response of an impulsively loaded circular ring is examined. The numerical stability criterion associated with a finite difference formulation of the problem is briefly discussed, and a method to reduce the stability restriction is presented. This method assumes that the density of the ring is greater in the tangential direction than it is in the radial direction. The analytical solution to the ring equations with the artificial tangential inertia is determined for a specific impulsive load. This solution is compared with the solution to the ring equations with the correct tangential inertia. The comparison shows that on the basis of predicting peak values of stress, the results for the ring with the artificial tangential inertia are very close to those of the unmodified ring. Thus, the method reduces the numerical stability requirements and does not significantly affect the principal results.

DD FORM 1 JAN 64 1473

14 KEY WORDS	LINK A		LINK B		LINK C	
	ROLE	WT	ROLE	WT	ROLE	WT
Elastic Rings						
Numerical Stability						
Finite Difference